Genomics-enhanced contact tracing enabled the improved characterization of SARS-CoV-2 transmission in outbreak settings and in the general population

Johannes Ptok[1,2#], Jonas Weber[1#], Moritz Pigulla[1,3#], Coco Röhl[1,3], Nils Lüschow[1], Dirk Nagels[3], Torsten Houwaart[1], Samir Belhaj[1,3], Lena-Sophie Schneider[1,3], Dominik Regorz[3], Pascal Kreuzer[3], Yara Fröhlich[3], Patrick Finzer[1,4], Emran Tawalbeh[3], Jessica Nicolai[1], Mygg Stiller[5], Jacqueline Blum[5], Christian Lange[5], Roland Geisel[5], Daniel Wind[1], Lisanna Hülse[1], Alona Tysha[1], Tobias Wienemann[1], Malte Kohns Vasconcelos[1,6], Katrin Hoffmann[4], Nadine Lübke[2], Sandra Hauka[2], Klaus Pfeffer[1], Jörg Timm[2], Lutz Ehlkes[3,&], Andreas Walker[2,&], Alexander T. Dilthey[1,7,&,*]

[1] Institute of Medical Microbiology and Hospital Hygiene, Heinrich Heine University Düsseldorf, Düsseldorf, Germany
[2] Institute of Virology, University Hospital Düsseldorf, Heinrich Heine University Düsseldorf, Düsseldorf, Germany
[3] Düsseldorf Health Authority (Gesundheitsamt Düsseldorf), Düsseldorf, Germany
[4] Zotz | Klimas, Düsseldorf, Germany
[5] Medizinische Laboratorien Düsseldorf, Düsseldorf, Germany
[6] Department for Epidemiology, Institute for Medical Biometry and Epidemiology, University Medical Centre Hamburg-Eppendorf, Hamburg, Germany
[7] Center for Digital Medicine, Heinrich Heine University Düsseldorf, Düsseldorf, Germany

# These authors are joint first authors
& These authors jointly supervised this work
* Address for correspondence: dilthey@hhu.de

Abstract

Understanding pathogen transmission is key to effective infection prevention. From February to December 2021, we implemented genomics-enhanced contact tracing for SARS-CoV-2 in Düsseldorf, Germany, integrating data on 32,380 cases, 49,906 contact tracing records, 162 outbreaks, and 8,028 viral genomes (sequencing coverage 24.5%). Combining epidemiological and genetic data, we found a putative infection source for 19% of sequenced and 44% of all cases. Household-associated transmission accounted for up to 40% of all cases; genetic links for epidemiologically unexplained cases suggested limited sensitivity of classical contact tracing for non-household links. Outbreaks were associated with 8% of cases; school, kindergarten and nightlife outbreaks were strongly connected to the community, with nightlife outbreaks showing a strong post-outbreak increase in genetically associated cases. Sequencing detected previously unrecognized links between school outbreaks and 18% additional outbreak-associated sequenced cases. Across analyses, schools, kindergartens and gastronomy and nightlife settings were consistently identified as important contributors to transmission dynamics.

Introduction

Understanding when, where and between whom pathogens are transmitted is the foundational question of infectious disease epidemiology. Knowledge of pathogen transmission patterns can contribute to the implementation of effective infection prevention measures. However, during community transmission, the structure of transmission chains and of the structural factors driving them – such as the contribution of outbreaks – often remains elusive to both the affected individual and the public health system. Reasons for this include the fact that there are often multiple potential sources for each individual infection event, which are not easily disambiguated; that some transmissions take place between individuals not known to each other, limiting the efficacy of classical contact tracing; and resource constraints at the level of public health systems, which limit the ability

to comprehensively track and investigate transmission chains and their associated infection contexts at the population level.

Pathogen genome sequencing can play an important role in the characterization of pathogen transmission [Harris et al. 2013, Andersen et al. 2015, Mate et al. 2015, Faria et al. 2016, Mellmann et al. 2016, COVID-19 Genomics UK (COG-UK) 2020, Lane et al. 2021, Hjorleifsson et al. 2022, McCrone et al. 2022]. When combined with classical contact tracing, pathogen genome sequencing can enable the tracking of individual transmission chains in the population during community transmission ("genomics-enhanced contact tracing"; Seemann et al. [2020], Hjorleifsson et al. [2022], Walker et al. [2022], Sivertsen et al. [2024], Bludau et al. [2025]). In this context, pathogen genome sequencing can be used to validate or disambiguate epidemiological links detected by routine contact tracing; enable the discovery of links missed by routine contact tracing by directing in-depth epidemiological investigation efforts (e.g., based on in-depth case interviews) to case pairs with otherwise unexplained high genetic similarity [Houwaart et al. 2022]; and contribute to the characterization of large-scale transmission patterns, such as quantifying the overall impact of outbreaks. The implementation of genomics-enhanced contact tracing requires high contact tracing and case sequencing rates; of note, neither pathogen sequencing by itself nor other modeling approaches (e.g. of individual-level mobility patterns, Pullano et al. [2020]) are sufficient to enable the tracking of individual transmission chains.

In 2021, the city of Düsseldorf, the capital of Germany's most populous federal state, implemented a system for genomics-enhanced contact tracing of SARS-CoV-2, which combined best-practice classical contact tracing with one of the highest-intensity SARS-CoV-2 genomic surveillance regimes in continental Europe [Houwaart et al. 2022, Walker et al. 2022]. Here, we report on the first retrospective analysis of the complete dataset (Fig. 1), with the specific aim of characterizing to which extent the integration of genetic data and classical contact tracing can enable insights into SARS-CoV-2 transmission chains that would not be obtained from classical contact tracing alone.

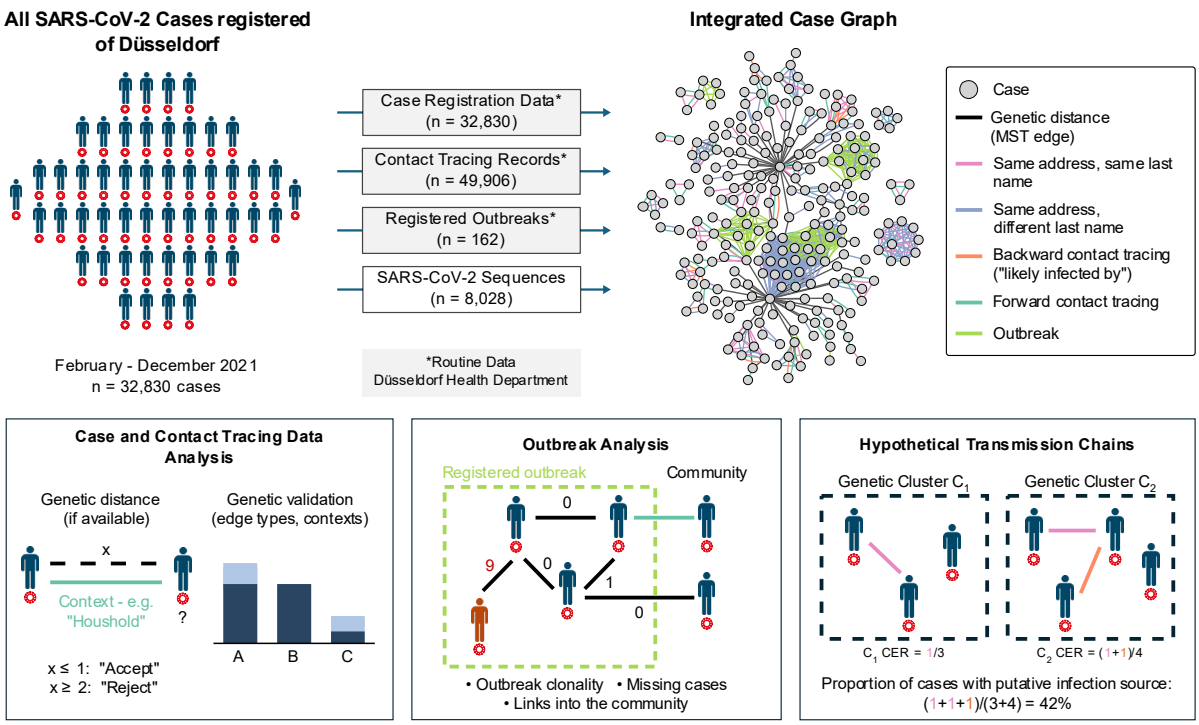

Figure 1: Characterization of the community transmission of SARS-CoV-2 based on genomics-enhanced contact tracing. Cases and their epidemiological connections, determined based on Düsseldorf Health Authority data, were represented in the form of an Integrated Case Graph. Genetic distance edges between sequenced cases are included for illustrative purposes; pairwise genetic distances are not stored as part of the graph. Based on the integrated dataset, we mapped epidemiological connections; investigated all registered institutional outbreaks; and attempted to identify a putative infection source for each registered case through hypothetical transmission chains (CER: cluster explanation rate). Across analyses, we used genetic data to evaluate whether epidemiological links between cases were likely associated with transmission.

Results

Implementation of genomics-enhanced contact tracing of SARS-CoV-2 in Düsseldorf

Between February and December 2021, the city of Düsseldorf implemented genomics-enhanced contact tracing for SARS-CoV-2. Best-practice classical contact tracing for all diagnosed SARS-CoV-2 cases from Düsseldorf was carried out by Düsseldorf Health Department, based on Germany's Law on the Prevention of Infection ("Infektionsschutzgesetz") and following guidelines of Germany's Robert Koch Institute; this involved (i) the registration of all detected cases and their personal data (n = 32,830 cases); (ii) contact tracing for all registered cases, with a minimum of three contact attempts using available landline or mobile phone numbers by Düsseldorf Health Authority personnel before contact tracing was deemed unsuccessful (n = 48,131 forward and n = 875 backward contact tracing records; Supplementary Figure 1 and Supplementary Figure 2); and (iii) the registration and investigation of suspected outbreaks in institutional settings such as schools (n = 162 outbreaks with 919 associated cases). Contact tracing was carried out in the context of a mitigation strategy that aimed to reduce, but not eliminate, infections. Rapid SARS-CoV-2 sequencing for as many local SARS-CoV-2 isolates as possible was carried out in collaboration between two large commercial diagnostic labs, Düsseldorf Health Authority, and Heinrich Heine University [Houwaart et al. 2022, Walker et al. 2022]. The collected sequencing data (Fig. 2A; Supplementary Table 1) comprised n = 11,349 collected viral genome sequences, of which n = 8,763 passed quality control with <= 3,000 ambiguous or undefined nucleotides. The median turnaround time from sample arrival at Heinrich Heine University to availability of a first sequence was 63 hours (tracked for a subset of the samples collected between April and June 2021; Supplementary Fig. 3). All personally identifiable data remained at Düsseldorf Health Authority.

Unified representation of all epidemiological and genomic data in the Integrated Case Graph

We developed a scalable data integration approach to enable the analysis of the collected data. Case, contact tracing and pathogen genome sequencing data were represented in the form of an Integrated Case Graph (Fig. 1), in which cases were represented as nodes; epidemiological connections between cases were represented as edges; and pathogen genome sequences were attached to the nodes of their corresponding cases (Methods, Supplementary Fig. 4). The included epidemiological connections were established based on i) forward and backward contact tracing interviews; ii) assignment of cases to the same outbreak; and iii) the registered address and last name data of cases, inducing an epidemiological edge between two case nodes if the cases were registered at the same address and shared, or did not share, the same last name (the corresponding edge types are referred to as "sameAddress-sameName" and "sameAddress-differentName", respectively). We established record linkage between cases and n = 8,763 SARS-CoV-2 genome sequencing records after quality control based on available metadata and manual curation if necessary; for cases with more than one sequenced viral isolate from the same infection, a single sequence was selected, resulting in 8,028 cases with viral genomes available (Methods). The overall proportion of sequenced cases was 24.5%;

the proportion of sequenced cases varied between 7.9% and 50.4% on a weekly basis (Fig. 2a, Supplementary Table 2) and the sequenced viral genomes were dominated by the Alpha, Delta, and Omicron variants [Rambaut et al. 2020], depending on the time of the year (Supplementary Figure 5). The Integrated Case Graph comprised 32,830 case nodes, 8,028 viral genome sequences, and 39,927 links between pairs of cases (edges). The majority of connections between cases were accounted for by "sameAddress"-type edges (65.6%), followed by forward contact tracing edges (20.5%), edges connecting cases in outbreaks (11.7%), and backward contact tracing edges (2.2%; Fig. 2b).

Forward and backward contact tracing connections, as well as "sameAddress"-type edges, exhibited genetic validation rates (genetic distance ≤ 1) of approximately 80%, whereas "outbreak" edges showed a genetic validation rate of 70% (Fig. 2c, Fig. 2d, Supplementary Figure 6). A set of randomly scrambled contact tracing links (Methods) showed a markedly different distribution of genetic differences (average genetic distance 21; Supplementary Fig. 7e), confirming that the observed genetic distance distribution for the real epidemiological links did not result from incidental genetic similarity between cases sequenced at approximately the same time. The contact tracing connections in the graph mainly represented household-associated transmission (84%); household-associated transmission also accounted for the majority (59%) of registered contacts (independent of whether they led to a transmission or not) and exhibited the highest context-specific transmission rate of infection contexts captured by contact tracing (30%; Supplementary Table 3; Supplementary Figure 8). "Private household" and "recreational context", the infection contexts with the highest frequency in the forward contact tracing data, did not significantly differ with respect to genetic validation (82% compared to 86%; p = 0.42, Fisher's Exact Test; Supplementary Figure 9).

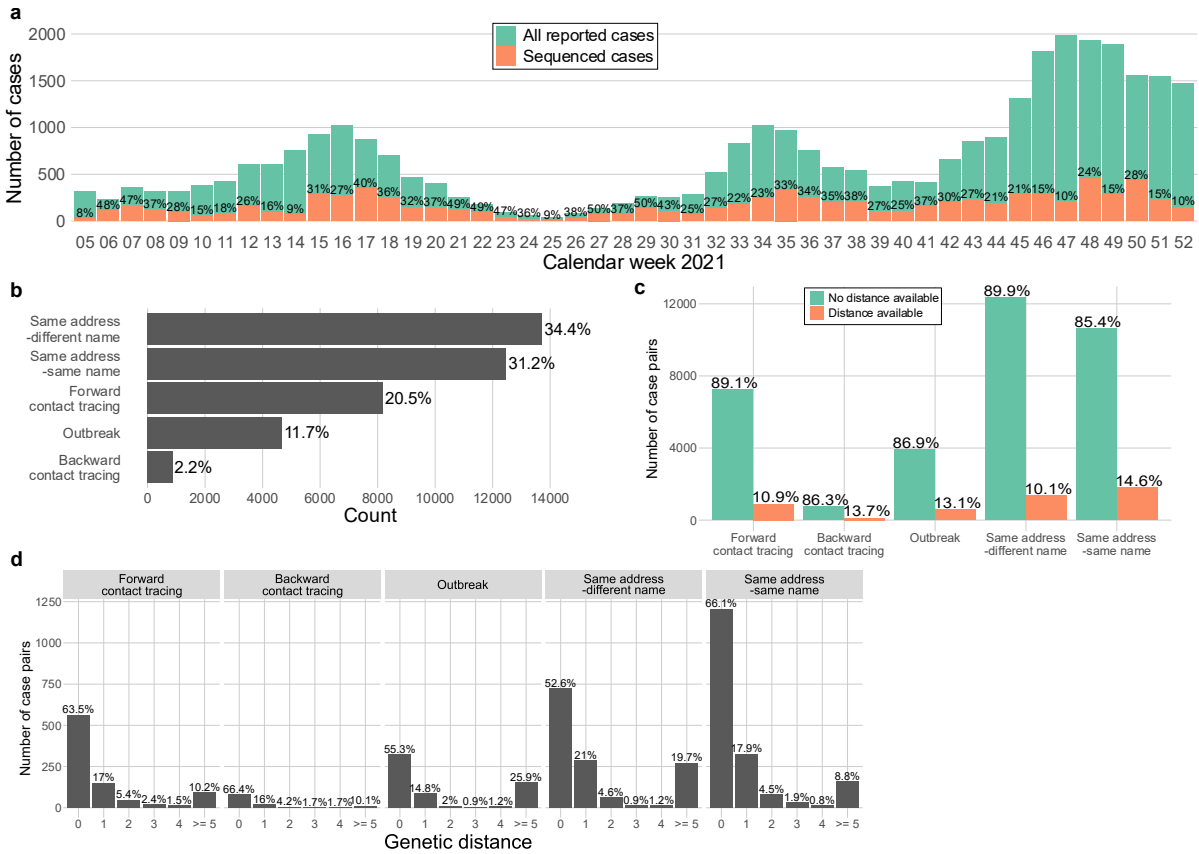

Figure 2: SARS-CoV-2 sequencing and epidemiological connections represented in the Integrated Case Graph. a, Shown is the number of registered and sequenced SARS-CoV-2 cases in Düsseldorf on a weekly basis between

February and December 2021. **b,** Edges in the Integrated Case Graph, stratified by edge type. **c,** Number of case pairs connected by different types of links in the Integrated Case Graph; shown in red is the proportion of case pairs for which a genetic distance was, based on the sequencing status of the corresponding cases, available. **d,** Distribution of SARS-CoV-2 genetic distances for case pairs linked by different types of edges in the Integrated Case Graph, stratified by edge type and only shown for case pairs for which a genetic distance was available. **e,** Infection contexts captured by forward contact tracing (case pairs with genetic distances only). Shown is the number of case pairs that were connected by a forward contact tracing edge assigned to the corresponding putative context, stratified by whether the genetic distance between the connected cases was ≤ 1 ("accepted") or > 1 ("rejected").

Household-associated transmission dominated explained infections, but classical contact tracing lacked sensitivity for other infection contexts

First, we set out to characterize how well we could explain SARS-CoV-2 transmission in the general population based on the collected data. We first focused on explicitly traced contacts (forward and backward contact tracing, as well as "outbreak"-type connections) within the set of sequenced cases. We clustered sequenced cases by genetic similarity (genetic distance threshold $t_g = 0$; n = 1,206 clusters; Supplementary Figure 10) and constructed hypothetical transmission chains (Fig. 3a) from the detected links between cases for each cluster, only allowing for connections between cases that were genetically supported and consistent with respect to symptom onset of the connected cases (i.e. $t_d = 0$; Methods) or relying on the given directionality of transmission assessed during backward contact tracing. Using only forward and backward contact tracing data, the constructed chains implied a putative infection source for 12% of cases in clusters (referred to as "Cluster Explanation Rate" or "CER") and 7% of all sequenced cases; also including "outbreak"-type edges increased the CER to 14% and the proportion of sequenced cases with a putative infection source to 8% (Fig. 3b).

The fact that the genetic validation rate of "sameAddress"-type edges was comparable to that of contact tracing edges indicated that these proxy indicators of joint household membership captured relevant epidemiological relationships. We therefore re-computed hypothetical transmission chains including "sameAddress"-type links, observing an increase in the CER to 31% and in the proportion of sequenced cases with an infection source to 19%. Within the computed chains, 91% of utilized connections were household-associated (Fig. 3c), translating to 28% of sequenced cases in genetic clusters with a household-associated infection source. These results were robust (Supplementary Table 4) to using different thresholds for genetic distance ($t_g = 1$), the symptom onset date difference ($t_d = 3$), and allowing for one or two intermediate non-sequenced cases ($t_j = 1/2$); the computed CERs were also relatively similar for different cluster sizes and over the study period (Supplementary Figure 11). $t_d = 0$ was chosen to enrich the set of considered edges for true-positive transmission events, excluding an expected 75% of edges with incorrect directionality of transmission according to a Bayesian analysis based on backward contact tracing (Supplementary Figure 12), while retaining an expected 89% of edges with correct directionality. $t_d = 3$, by contrast, represented a higher expected proportion of edges with correct directionality retained (99% in expectation), while the removal of edges with incorrect directionality was less stringent (46%; Supplementary Figure 12).

To investigate to which extent the computation of hypothetical transmission chains was constrained by the fact that it was carried out within the subset of sequenced cases, we treated the complete Integrated Case Graph of all n = 32,830 cases as one large cluster of genetically identical cases. This led to a substantial increase in the proportion of cases for which a potential infection source could be identified (44.4%; Fig. 3b), with 89% of putative transmissions being household-associated (Supplementary Table 5). However, more than half of cases remained without a plausible infection source, indicating that many transmission-relevant epidemiological connections within the city

population were not captured by classical contact tracing (as also suggested by the very large proportion of apparent household-associated transmission), and/or substantial importation of cases.

We used genetic data to gain further insights into missed epidemiological links. Transmissions within the city population would be associated with low genetic distances between cases; imported infections, by contrast, would typically exhibit increased genetic distances. We therefore re-computed hypothetical transmission chains assuming that all genetically linked samples were also epidemiologically connected. For $t_g = 0$, the proportion of sequenced cases with a defined infection source increased to 43.9%; for $t_g = 1$, it increased to 60.5%, consistent with the hypothesis that a substantial number of epidemiological links within the city population were missed by contact tracing (Fig. 3b). To identify the infection contexts that may contribute to these, we labeled each sequenced case with the contexts of all contacts detected for the case during forward contact tracing (independent of whether the traced contact was associated with a transmission or not). For each context and the corresponding sequenced cases, we then determined the average number of genetically linked cases (genetic distance $= 0$ and difference in registration in dates $\leq$ 14 days) and compared it to the average number of classically traced contacts within the set of sequenced cases (Fig. 3d). While cases with contacts in the "private household" category had approximately 1.4 as many genetically linked cases as classically traced contacts, cases with contacts in the gastronomy, hospital, school and kindergarten contexts had 3 – 6 times as many genetically linked cases, suggesting that these contexts were enriched for infection-associated contacts not captured by classical contact tracing.

In conclusion, based on high-confidence sequencing-supported hypothetical transmission chains and transmission chains computed based on only epidemiological connections, we found a potential infection source for 19% of sequenced and 44% of all cases, respectively; at approximately 90%, household-associated transmission dominated both sets of transmission chains, implying a household-associated infection source for up to 40% of all cases. Classical contact tracing had limited sensitivity for non-household contacts; analysis of sequencing data enabled the identification of infection contexts that were likely enriched for undetected transmissions.

.

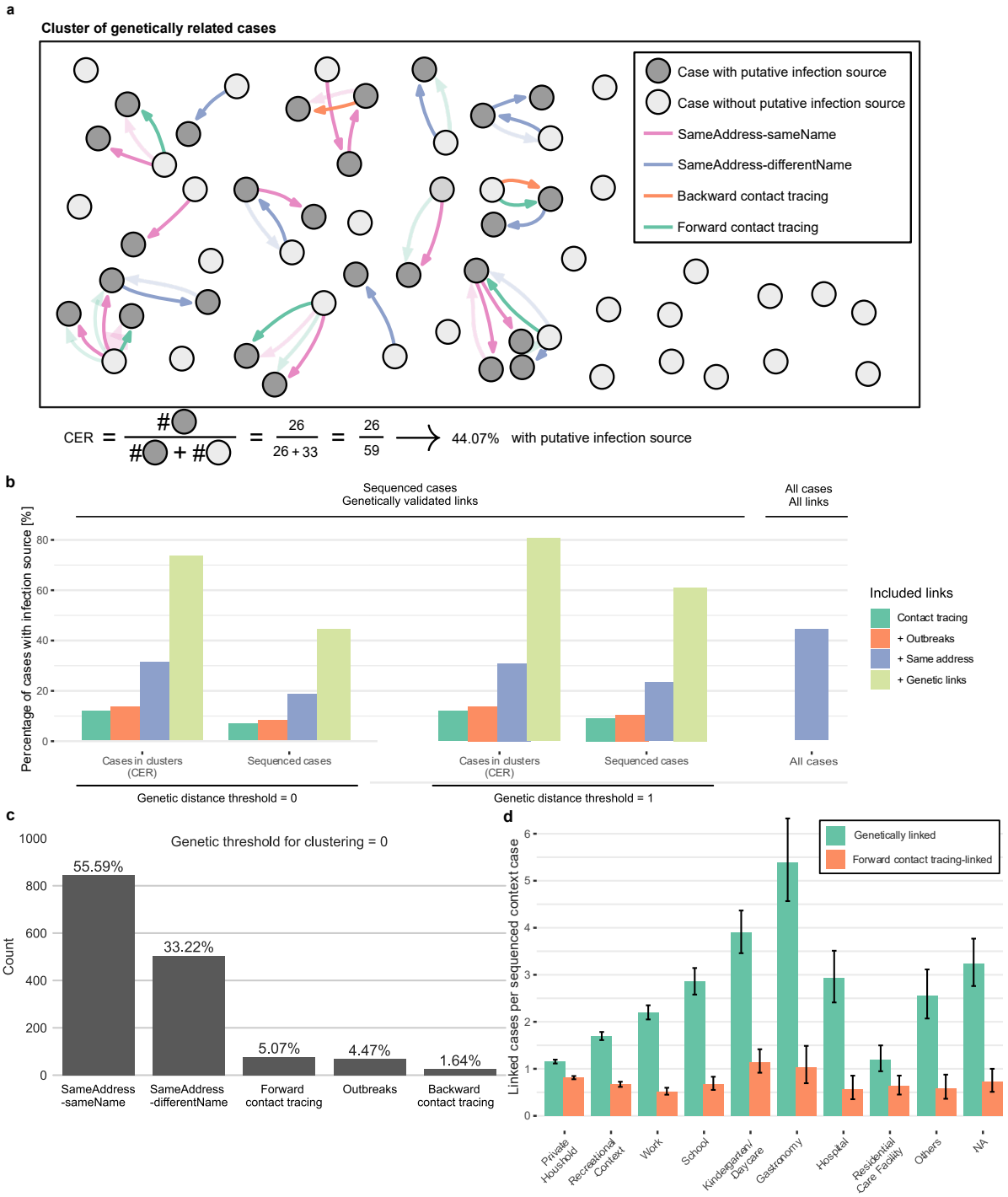

Figure 3: Integrated characterization of SARS-CoV-2 community transmission. a, Visualization of a real cluster of genetically related cases (cluster "27" of the $t_g = 1$ $t_d = 0$, $t_j = 0$ cluster computation; see Supplementary Table 6) and illustration of the CER computation. Nodes correspond to cases and edges to epidemiological connections of different types (after directionalization). Edges rendered with full opacity are part of the hypothetical transmission chain computed for the cluster; faded edges were not selected. We manually added 4 edges to illustrate that some case pairs maintain bidirectional links after directionalization. **b,** Proportion of cases with a putative infection source, stratified by case sequencing and cluster membership status and based on hypothetical transmission chains (see Methods) computed based on genetic clustering similarity thresholds t_g of 0 and 1 and. **c,** Edges contained in the computed hypothetical transmission chains for $t_g = t_j = 0$ and $t_d = 0$, stratified by edge type. **d,** Average number of genetically linked cases (genetic distance 0 and difference in registration in dates ≤ 14 days) compared to the average number of sequenced cases linked via classical contact tracing for cases with contacts of the given category.

Institutional outbreaks were associated with approximately 8% of overall SARS-CoV-2 case load and different impacts on community transmission

Next, we focused on SARS-CoV-2 outbreaks, characterizing transmission both within outbreaks and between outbreaks and the community. We analyzed all n = 162 institutional outbreaks with 919 associated cases recorded in Düsseldorf during the study period (Supplementary Table 7). The number of cases varied by outbreak category (Fig. 4a, Fig. 4b); 49 school outbreaks accounted for 230 registered cases, followed by 13 care home outbreaks accounting for 161 cases, and 23 outbreaks in kindergartens/daycares accounting for 121 cases; care home outbreaks had the highest number of cases per outbreak (mean = 12.4; Supplementary Table 8). To evaluate whether the outbreaks were genetically homogeneous and whether the assignment of individual cases to outbreaks was correct, we used genome sequencing data. In 48 outbreaks more than one sequenced case was present; of these, 37.5% (n = 18 outbreaks) were classified as not genetically homogeneous because they contained at least one case that was not closely related to the other outbreak cases (genetic distance threshold of ≤ 1; Methods); 12 outbreaks contained more than one SARS-CoV-2 Pango lineage. Based on a genetic distance threshold of ≤ 1, 15% (n = 31) of the 203 sequenced cases in the outbreaks with more than one sequenced case were found to be likely mis-assigned, i.e. not closely related to the other cases in their corresponding outbreak (Methods).

As a first-order measure of the role of outbreaks in the wider transmission network of SARS-CoV-2, we determined the number of community cases connected to outbreaks (represented by any one of their cases) via links of type contact tracing and "sameAddress" in the Integrated Case Graph. 659 community cases were found to be epidemiologically linked to at least one outbreak (Fig. 4c), accounting, when combined with outbreak cases, for approximately 5% of cases in Düsseldorf over the considered period. Of the identified outbreak-linked cases, 22% (n = 150 / 659) could be evaluated genetically based on the availability of a genetic distance between the outbreak-linked case and any one outbreak case; of these, 65% (n = 98 / 150) were confirmed based on a genetic distance of ≤ 1. Schools and kindergartens combined accounted for approximately two thirds of overall and sequencing-confirmed linked cases (Supplementary Table 8); these two outbreak types also had the highest number of linked community cases per outbreak case (5.9 and 6.2, summed over all school and kindergarten outbreaks; Supplementary Table 8, Supplementary Figure 13 L). By contrast, care homes exhibited the lowest proportion of linked community cases relative to registered outbreak cases (average = 0.2; Supplementary Table 8) and were therefore, despite high overall case count, associated with a relatively low absolute number of linked community cases. "sameAddress"-type links accounted for 1.7 times as many overall and approximately twice as many sequencing-confirmed linked community cases as contact tracing-implied links, respectively (Supplementary Table 8).

As an orthogonal measure of the connectedness between outbreaks and the community that was not affected by potential biases of classical contact tracing, we also determined the number of community cases that were, within a two-week time window, genetically linked to an outbreak (Fig 4d; Methods). In total, 1,000 community cases were found to be linked to an outbreak. Of these, 94% did not exhibit an epidemiological link to the outbreak they were genetically linked to, increasing the total proportion of outbreak-associated cases (outbreak cases plus genetic and epidemiological links) to 8%. School and nightlife outbreaks were associated with the largest number of genetically linked community cases (n = 243 and n = 200, respectively; Supplementary Table 5); nightlife outbreaks also had the highest number of genetically linked community cases when normalized by outbreak size (Supplementary Table 8, Supplementary Figure 13). To assess the potential role of outbreaks as drivers of community transmission, we stratified the genetically linked community cases by whether they were registered before, during or after their associated outbreaks (Fig. 4e); to avoid confounding by

variant-associated growth effects, we removed 8 outbreaks that were associated with the Delta and Omicron variants and that overlapped, with their surrounding 2-week windows, with the expansion phases of these variants (before week 29 for Delta and all 4 Omicron outbreaks in weeks 48 to 51; see Supplementary Figure 5). Nightlife outbreaks in particular were associated with a four-fold increase in the number of associated cases in the post- compared to the pre-outbreak period; schools and kindergartens, with an approximately two-fold increase. Care homes, by contrast, were associated with a comparatively low number of genetically linked post-outbreak cases.

In summary, outbreaks were associated with 8% of total cases. The outbreak documentation carried out by Düsseldorf Health Authority according to best-practice guidelines was largely correct, with only 15% of cases found to be misassigned based on genetic data. Using classical epidemiological and genetics-based measures, we found that school, kindergarten, and nightlife outbreaks were strongly linked to the community and associated with a post-outbreak increase in genetically linked cases, indicating that these likely contributed to driving community transmission. Care homes, by contrast, were only weakly linked epidemiologically and had a lower number of post-outbreak cases, indicating a less important role of these in driving community transmission. The high degree of community connectedness of nightlife outbreaks was only apparent in the genetic analysis, indicating that classical outbreak control and investigation approaches were less effective for these.

.

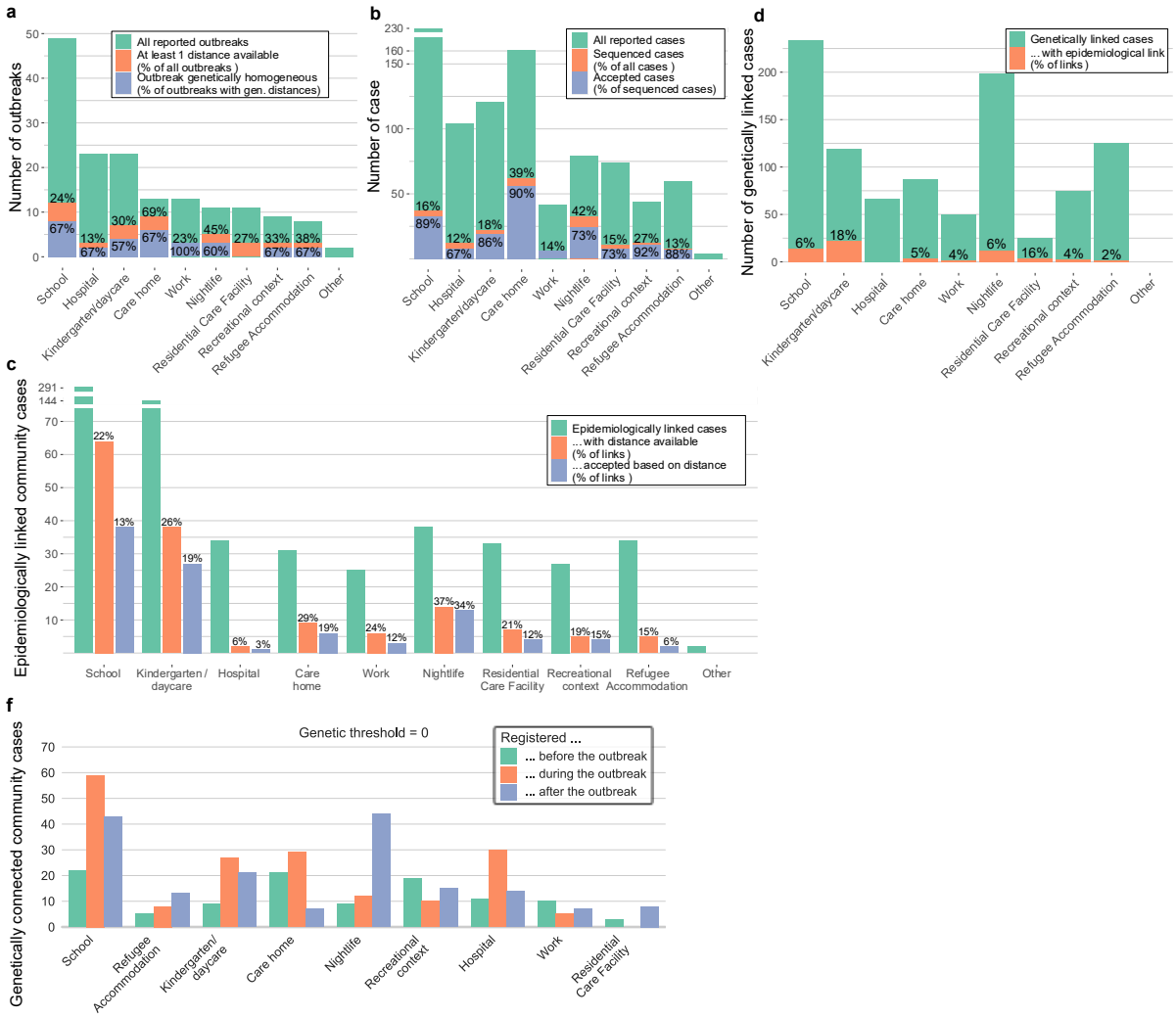

Figure 4. Genomics-based investigation of SARS-CoV-2 outbreaks and their links into the community. a, SARS-CoV-2 outbreaks by outbreak type; also shown is the proportion of outbreaks in the respective category with ≥2 sequenced cases and the proportion of outbreaks classified as genetically homogeneous based on a genetic distance threshold of ≤1 (see Methods). **b,** SARS-CoV-2 cases in outbreaks by outbreak type; also shown is the proportion of sequenced cases in the respective outbreak category and the proportion of sequenced cases in the corresponding outbreak category classified as "accepted" (i.e., part of the largest genetic cluster in the outbreak, based on a clustering threshold of ≤1; Methods). **c,** Cases epidemiologically linked to outbreaks, by outbreak type; also shown is the proportion of epidemiologically linked cases in the corresponding outbreak category for which a genetic distance to their associated outbreak could be computed, and the proportion of such cases for which the computed distance was ≤1 ("accepted"). The genetic distance between a case epidemiologically linked to an outbreak and the outbreak was defined as the minimum genetic distance between the linked case and any case of the outbreak; computation of a such a distance was possible if the outbreak contained at least one sequenced case and if the linked case itself was sequenced. **d,** Cases genetically linked to outbreaks (genetic distance 0, case registration date difference ≤ 14 days), by outbreak type; also shown is the proportion of genetically linked cases that also exhibited an epidemiological link to their corresponding outbreak. **e,** Cases genetically linked to outbreaks and stratified by outbreak type and relative case registration date; 8 outbreaks that were associated with the Delta and Omicron variants and that overlapped, with their surrounding 2-week windows for the inclusion of linked variants, with the expansion phases of these variants were not included.

In-depth manual analysis of school outbreaks identified additional outbreak-linked cases and links between outbreaks

To assess whether genetic data could contribute to the discovery of epidemiological connections not captured by routine contact tracing, and to investigate the potentially important role of schools for SARS-CoV-2 transmission, we carried out an in-depth manual investigation of SARS-CoV-2 transmission within the n = 49 registered school outbreaks and their links to the community (Supplementary Table 8; Supplementary Table 7). We (i) manually reviewed the complete Düsseldorf Health Department database records of all relevant cases and (ii) searched for additional outbreak-linked community cases based on genetic data (Methods; Supplementary Figure 14). According to routine contact tracing, the investigated outbreaks comprised 226 cases, of which 51 were sequenced and 4, based on genetic distances, falsely assigned (i.e. not part of the outbreak they were assigned to by routine contact tracing); as well as epidemiological links to 291 community samples, of which 38 were genetically validated (Fig. 5a).

First, we carried out a search for additional outbreak-linked cases. In some instances, free-text database entry fields were used to record the results of contact tracing interviews; we evaluated whether contacts recorded in these (i.e., in a non-structured manner and thus not amenable to automated extraction) increased the number of outbreak-linked community cases, but found only a single instance of a non-structured contact tracing record implying a link between a community case and a school outbreak that was not already represented in the Integrated Case Graph (via an edge of any type between the contact and any case of the associated outbreak). We turned to the analysis of genetic data for the identification of additional outbreak-linked cases and found 20 sequenced cases (Fig. 5a) that were not linked to a school outbreak in the Integrated Case Graph or mentioned in free-text contact tracing records, but for which a genetic link to a school outbreak (genetic distance threshold ≤ 1) could be epidemiologically confirmed through manual review of case database records, typically based on information found in other free-text entry fields. For example, in the analysis of outbreaks 0107 and 0108 (Fig. 5b), Case 24 was classified as outbreak-linked because it genetically clustered with the outbreaks and because the case was found to be a pupil at the school at which the outbreaks occurred, confirming an epidemiological link. In addition, we found 7 non-sequenced cases that were classified as outbreak-linked because they represented the "missing epidemiological link"

between an outbreak and a genetically linked third case (Fig. 5a, Methods); such as Case 23, which represented the only detected epidemiological link that could account for the observed genetic link between Case 38 and outbreaks 0107 and 0108 (Fig. 5b).

Second, we evaluated whether the assignment of cases to outbreaks was complete. We focused on n = 58 sequenced cases that were not registered as school outbreak cases according to the original outbreak documentation carried out by Düsseldorf Health Authority, but genetically and epidemiologically linked to a school outbreak (including the 20 genetically identified outbreak-linked cases described above). Of the 58 investigated cases, 11 met the criteria for being classified as outbreak cases – for example Cases 23 and 24, as pupils at the school at which outbreaks 0107 and 0108 occurred (Fig. 5b). Correct registration of the 11 cases would have increased the number of sequenced outbreak cases by 22% (compared to a baseline of 51 sequenced outbreak cases, of which at least 4 were misclassified according to genetic data; Fig. 5a and Supplementary Table 8).

Third, we investigated whether there were connections between separately registered school outbreaks and found that 8 school outbreaks were epidemiologically and genetically connected to at least one other school outbreak (Supplementary Table 9; Supplementary Note 1). Examples include the genetic and epidemiological links between outbreaks 0107 and 0108 (Fig. 5b), which were two separately registered multi-class outbreaks at the same school, as well as the detected links between the separately registered outbreaks 0212, 0231, and 0231 at the same school. Due to the detected epidemiological links, these, like the other outbreaks found to be linked in our analysis, should have been registered as single outbreaks.

In summary, the number of cases associated with school outbreaks was higher than initially estimated (18% increase when measured within the set of sequenced cases, Fig. 5b); the absolute number of school outbreak-associated cases, however, remained relatively low. Sequencing data enabled the discovery of additional relevant epidemiological connections that were not captured by the extracted Düsseldorf Health Authority routine data.

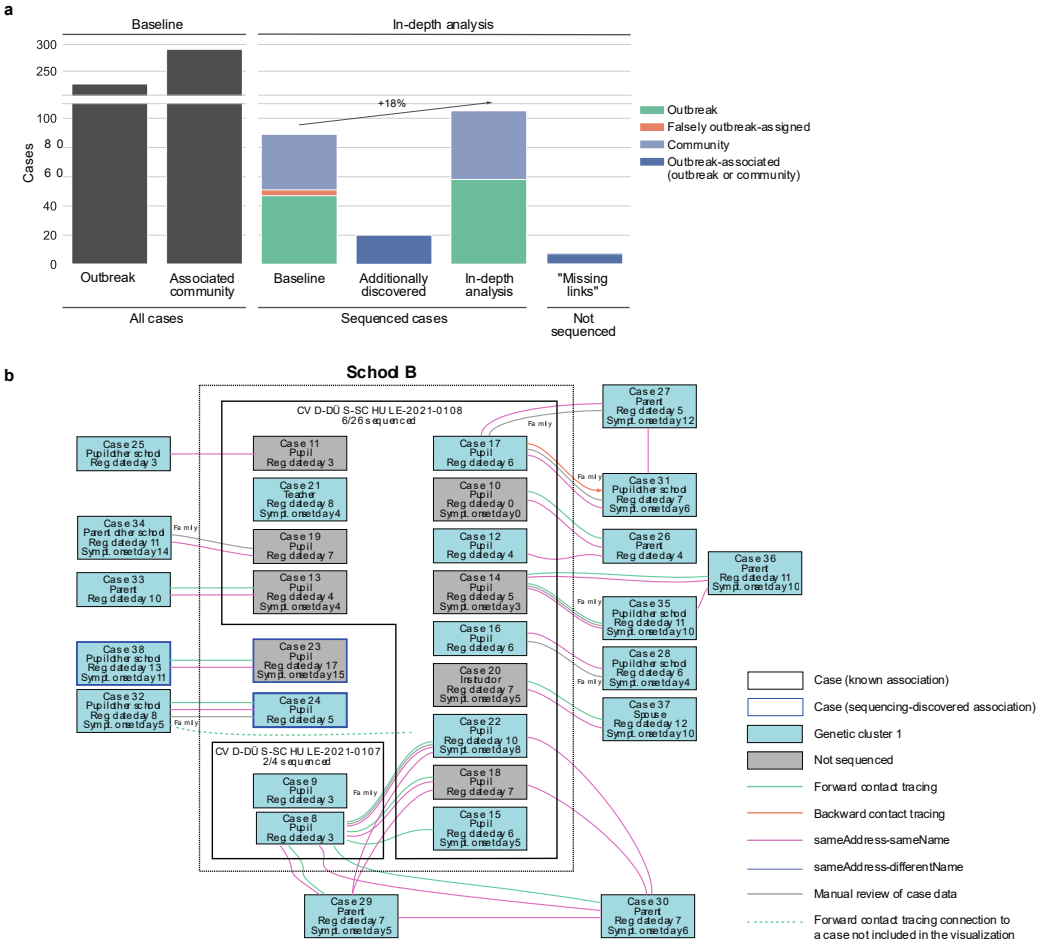

Figure 5. In-depth analysis of school outbreaks. a, School outbreak-associated cases before and after in-depth manual analysis. Black bars show the total number of school outbreak-associated cases before manual analysis and independent of sequencing status; colored bars show the results of in-depth analysis for the subset of sequenced outbreak-associated cases, as well as the number of non-sequenced cases that were classified as outbreak-linked because they represented the required "missing epidemiological link" between an outbreak and a genetically linked third case. **b,** Visualization of two school outbreaks (0107 and 0108), registered at the same school, and of the epidemiological links between the associated cases. All sequenced cases (boxes with blue background) were part of the same genetic cluster (see Supplementary Note 1 for a full genetic distance matrix); for outbreak 0108, only a subset of cases is shown. Cases 23, 24, and 38 were classified as outbreak-associated based on the analysis of genetic data; Case 23 is an example of a "missing epidemiological link" that was classified as outbreak-associated because it represented the only detected epidemiological link that could account for the genetic link between Case 38 and the two shown outbreaks.

High sequencing coverage was required for high-resolution characterization of transmission

Last, we asked which case sequencing coverage was required for genomics-enhanced contact tracing (Figure 6, Supplementary Figure 15, Supplementary Figure 16). We focused on four key areas for which our previous analyses demonstrated that sequencing could contribute to the improved characterization of SARS-CoV-2 transmission: (i) genetic validation of epidemiological connections (Fig. 6a); (ii) investigation of genetic homogeneity within outbreaks of their genetic links to the community (Fig. 6b and c); (iii) finding putative infection sources of individual cases from high-confidence sequencing-supported hypothetical transmission chains (Fig. 6d); and (iv) identification of infection contexts underrepresented in classical contact tracing and of outbreak types associated with an increase in post-outbreak genetically linked cases (Fig. 6e and f).

Downsampling the set of available SARS-CoV-2 sequences when actual pairwise genetic distances were required, or randomly increasing the proportion of sequenced cases otherwise, we found that higher case sequencing rates consistently enabled led to improved characterization performance. This applied both to indicators that measured the validation or detection of individual epidemiological connections, as well as to indicators that captured large-scale transmission patterns. For the context-specific comparison of genetically to epidemiologically linked cases, a sequencing rate of 15% recovered the results of the full analysis, identifying schools, kindergartens and gastronomy as likely underrepresented in classical contact tracing; at a sequencing rate of 10%, the confidence intervals for the corresponding contexts were still largely overlapping (Fig. 6e). For the analysis of post-outbreak cases, two of the three outbreak types identified in the full analysis (schools, kindergartens, nightlife) also exhibited a clear increase in the count of post-outbreak cases at a sequencing rate of 15%; at 10%, absolute case numbers were much smaller and an increase was visible, but less pronounced (Fig. 6 e). A sequencing rate of 15% would thus have been sufficient to recover the majority of results about non-household transmission dynamics.

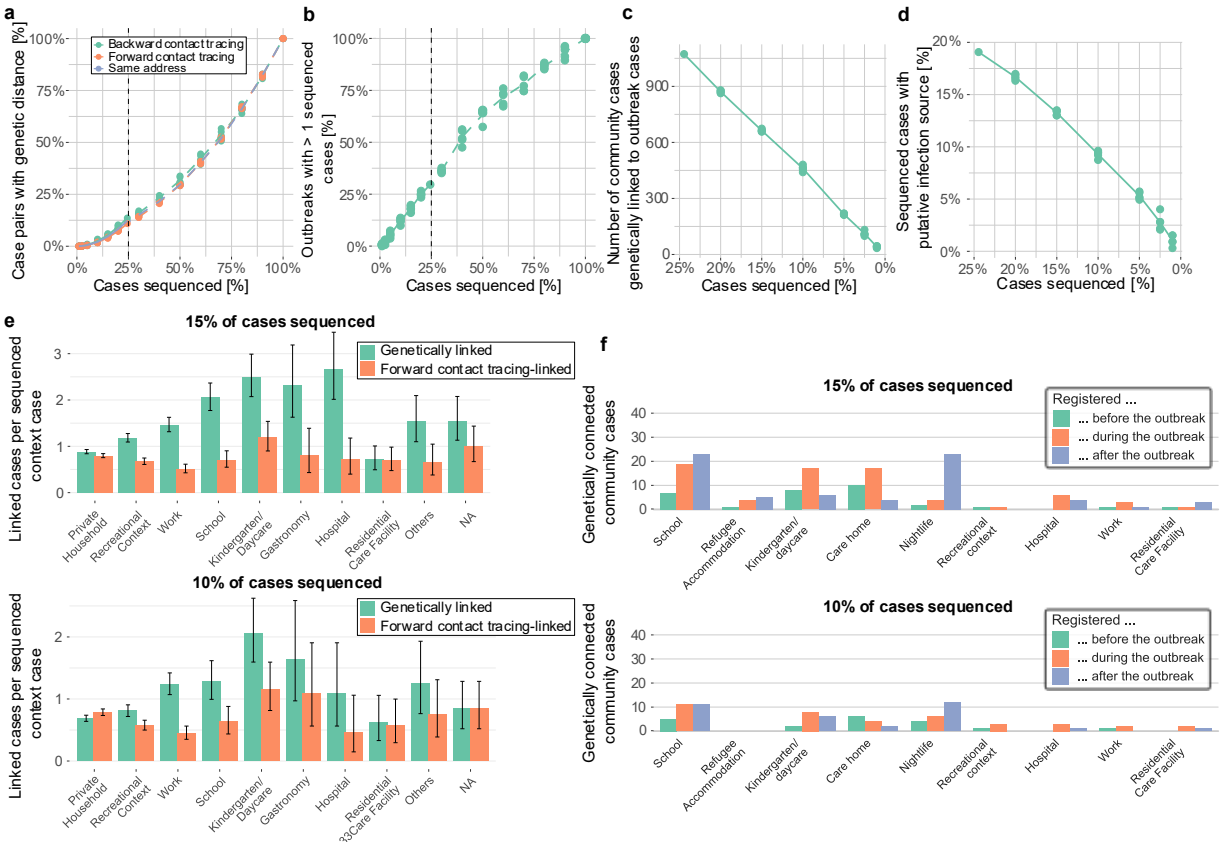

Figure 6: Influence of the proportion of sequenced cases on the ability to characterize SARS-CoV-2 transmission. a, Proportion of edges in the Integrated Case Graph that could be genetically validated at different case sequencing rates (5 replicates), shown for different edge types. **b,** Proportion of registered outbreaks that could be genetically validated (based on > 1 sequenced outbreak case, 5 replicates). **c,** Number of community cases genetically linked to outbreaks (5 replicates). **d,** Proportion of sequenced cases with a putative infection source, based on hypothetical transmission chains re-computed for each replicate (5 replicates). **e,** Average numbers of genetically linked and sequenced cases linked via classical contact for cases with contacts of the given category at different case sequencing rates; see Fig. 3d for results based on the complete data. **f,** Cases genetically linked to outbreaks, stratified by outbreak type and relative case registration date, at different case sequencing rates; see Fig 4e for results based on the complete data.

Discussion

In 2021, we carried out one of the highest-intensity SARS-CoV-2 integrated genomic surveillance programmes in continental Europe and implemented genomics-enhanced contact tracing (Fig. 1, Fig. 2). The resulting data set of more than 30,000 cases, almost 50,000 contact tracing records, and 8,000 viral genomes represents a rich resource on the structure of SARS-CoV-2 community transmission in an internationally connected city and against the backdrop of a public health mitigation strategy. We used the collected data to characterize SARS-CoV-2 transmission in the general population and in and around outbreaks under these conditions.

To characterize transmission in the general population, we used the combined epidemiological and genetic data in the Integrated Case Graph to reconstruct hypothetical transmission chains of SARS-CoV-2. We found a potential infection source for 19% of sequenced and 44% of all cases, respectively, with household-associated transmission accounting for up to 40% of all cases. Many cases that remained unexplained based on the available epidemiological links had close genetic links to other cases, suggesting that classical contact tracing had likely missed many relevant epidemiological connections. Contact-tracing informed analysis of genetic data, however, enabled insights into these, showing that cases with contacts in the gastronomy, hospital, school and kindergarten contexts were enriched for genetic compared to contact tracing-based links, thus suggesting a more important contribution of these contexts to overall transmission dynamics than would be assumed based on classical contact tracing alone. The availability of sequencing data played a key role in validating epidemiological links, supporting the inclusion of “sameAddress”-type links (which accounted for the majority of detected infection sources and connected a substantial number of cases not otherwise connected; Supplementary Figure 17) alongside explicitly traced contacts, and in the identification of epidemiological contexts likely enriched for undetected transmissions.

To characterize transmission in and around outbreaks, we relied on the set of 162 institutional outbreaks detected by Düsseldorf Health Authority. We investigated the connectedness between outbreaks and the community using epidemiological and genetic indicators and found differences between outbreak types. Schools, kindergartens and nightlife outbreaks exhibited a high, and care homes a relatively low, degree of linkage to the community. In a targeted analysis of school outbreaks, we found previously unrecognized connections between outbreaks and showed, at the level of manually confirmed epidemiological connections, that routine classical contact tracing had underestimated the number of outbreak-associated cases (19% increase within the set of sequenced cases). At a sequencing coverage of 24.5%, additional cases connected to school outbreaks almost certainly remained undiscovered; fully resolving the controversial role of schools [Lordan et al. 2021, Amodio et al. 2022, von Bismarck-Osten et al. 2022, Neil-Sztramko et al. 2024] would likely have required a higher case sequencing rate. For nightlife outbreaks, time-stratified analysis of genetically connected community cases suggested a particular effect of these in driving post-outbreak community transmission. Sequencing data played a key role in confirming the correct registration of the investigated outbreaks as mostly genetically homogeneous, enabling the detection of novel outbreak-connected cases and of connections between outbreaks, and in providing orthogonal measures of the connectedness between outbreaks and the community that did not depend on classical contact tracing.

In summary, under the epidemiological background conditions of our study, households accounted for a substantial, but less than half, proportion of overall transmission, while outbreaks were connected to approximately 8% of cases. Classical contact tracing showed low sensitivity for non-household contacts and failed to capture the full extent of the connectedness between outbreaks and the community. With respect to non-household infection contexts, both arms of our analysis

consistently identified schools, kindergartens and gastronomy and nightlife settings as potentially playing an important role in transmission dynamics. Care homes, by contrast, displayed a low degree of epidemiological connectedness to the community in outbreak analyses; of note, however, for the limited number of cases with contacts in the care home category (n = 14), we found a relatively high proportion of genetically to contact tracing-linked cases.

A similar proportion of household-associated transmission was observed based on digital contact tracing [Ferretti et al. 2024], during Iceland's first SARS-CoV-2 wave once the impact of travel-imported infections had been replaced by endogenous transmission [Gudbjartsson et al. 2020], and in other epidemiological studies [Manica et al. 2023]. Surveys of contact patterns [Mossong et al. 2008], including surveys of contact patterns carried out in Germany during the pandemic [Phuong et al. 2025], and digital contact tracing [Ferretti et al. 2024] indicated that household contacts were overrepresented by at least a factor of 2 in our dataset, consistent with the interpretation that gaps in contact tracing accounted for a substantial fraction of unexplained cases. Complementing these studies, we could identify specific infection contexts likely enriched for transmission events based on genetic data. Outbreaks [Leclerc et al. 2020, Wong et al. 2020] have been identified as associated with SARS-CoV-2 transmission, but most existing analyses described individual outbreaks [Allen et al. 2022, Nicolai et al. 2025]; relied on epidemiological modelling [Rodiah et al. 2023]; or did not have access to genomic data to validate the association of cases to individual outbreaks [Manica et al. 2023, Garcia-Bernardo et al. 2024]. Our study complemented these by providing a comprehensive characterization of SARS-CoV-2 transmission in and around outbreaks based on a large data set of more than 150 institutional outbreaks registered a single city and employing a combination of epidemiological and genetic approaches.

The results presented here also extend the existing literature on genomics-enhanced contact tracing in important ways. Whereas most previous successful implementations [Gudbjartsson et al. 2020, Seemann et al. 2020, Lane et al. 2021, Hjorleifsson et al. 2022, Hall et al. 2023] were carried out in the context of island nations with the ability to effectively control viral importations, relatively low incidences, and highly effective contact tracing carried out to support a public health viral elimination strategy, our study was carried out in the epidemiologically more open context of a single city in a large metropolitan area, under conditions of relatively higher incidences, and against the backdrop of a public health mitigation strategy that used contact tracing to reduce, but not eliminate, infections. Our study thus showed that genomics-enhanced contact tracing could be successfully implemented under these conditions, broadly representative of the current or expected conditions in many non-island localities during a pandemic or major outbreak. Compared to other implementations of genomics-enhanced contact tracing, lower sensitivity for non-household contacts limited our ability to identify individual infection sources. However, we could demonstrate the fine-scale characterization of transmission in and around a substantial number of outbreaks outbreaks, the frequency and relative importance of which increase under conditions of higher incidences.

The availability of large-scale sequencing data contributed to the pandemic public health response on multiple levels. First, sequencing confirmed that the core activities of Düsseldorf Health Authority during the pandemic – contact tracing and outbreak investigation – had a high genetic validation rate, providing internal quality control and implicitly validating the implemented contact tracing framework (based on guidelines by Germany's Robert Koch Institute). Second, the improved characterization of outbreaks could inform the implementation of improved infection prevention measures. For example, in the aftermath of the sequencing-informed investigation of a large nightlife outbreak [Houwaart et al. 2022], Düsseldorf Health Authority implemented a more stringent regime of monitoring the compliance of the affected bars with mandatory infection prevention measures. Third, sequencing

could help prioritize high-risk transmission settings for in-depth tracing and investigation activities. Based on the results presented here, improved surveillance in e.g. nightlife and gastronomy contexts may be particularly important. Last, sequencing could contribute to an improved calibration of policy decisions via evidence generation, e.g. by informing decisions on school closures with more accurate information on contribution of schools to overall community transmission, and to maintaining public support for public health measures, e.g. through demonstrating the high precision of classical contact tracing. Of note, large-scale sequencing in a public health context could be implemented with moderately low turnaround times; as demonstrated here, turnaround times of generally < 1 week (Supplementary Figure 3) were sufficient to successfully implement genomics-enhanced contact tracing in a retrospective manner. Additional applications, enabled by even lower turnaround times, may include e.g. the detection of active infection clusters in real time.

With respect to future implementations of genomics-enhanced contact tracing, our results imply that the characterization of transmission dynamics in outbreaks and the general population benefits from a sequencing rate of at least 15%; even higher sequencing rates may be required for a fine-scale characterization of transmission at the level of individual transmission chains in and around outbreak contexts of particular public interest , e.g. schools. Large language models may contribute to investigating sequencing-indicated links between cases in a scalable manner, e.g. through automated in-depth case interviews. Last, increased reliance on household membership information instead of explicit tracing of household contacts may free up resources for intensified surveillance and investigation in other epidemiological contexts. Genomics-enhanced contact tracing may thus provide the necessary information to navigate difficult societal trade-offs that arise in pandemic situations and enable an in-action as well as after-action evaluation of non-pharmaceutical interventions.

In conclusion, we demonstrated the successful implementation of genomics-enhanced contact tracing for SARS-CoV-2 under the conditions of high-incidence community transmission in a non-isolated geographical entity and showed that the integration of sequencing yielded information relevant outbreak control, infection prevention and public health policy. Our study thus informs future implementations and applications of genomics-enhanced contact tracing.

Limitations of this study: A link between two cases in the constructed hypothetical transmission chains does not imply an actual transmission event; in particular when computed independent of genetic data, the proportion of cases with a potential infection source should be interpreted as an upper bound on the ability to explain individual cases with the available epidemiological data. Edges of type “sameAddress” are imperfect indicators of joint household membership and edges of type “sameAddress-differentName”, in particular, may also sometimes capture transmission in e.g. residential facilities or large building complexes (Supplementary Figure 18, Supplementary Figure 17). Non-Düsseldorf contacts could not be analyzed in our study; however, non-Düsseldorf contacts only accounted for 19% of overall contacts and their improved analysis would, given the limited role of forward contact tracing-induced edges in the computed hypothetical transmission chains, likely not have led to a significant increase in the proportion of cases with a potential infection source or different conclusions with respect to infection contexts. Household contacts were substantially overrepresented in the collected forward and backward contact tracing data and confounding by other epidemiological factors could not be ruled out in the contact tracing informed-analyses of genetic data. The case sequencing coverage in our study was only 24.5%; increasing the proportion of sequenced cases while keeping the available contact tracing information constant might have led to an increase in CERs and in the proportion of cases with a potential infection source, but not beyond the 44.4% reported above for the complete Integrated Case Graph. Our study was based on data collected over a period of 11 months in 2021 and our results may not generalize to viral variants of

SARS-CoV-2 not covered by the study period, which may exhibit different transmission properties. Our analysis did not incorporate a potential effect of vaccination on SARS-CoV-2 transmission. Finally, the generalizability of the results to other respiratory pathogens beyond SARS-CoV-2 is an important direction for future research.

Supplementary Figure Legends

Supplementary Figure 1: Forward and backward contact tracing. a, Histogram over the number of registered forward contact tracing records per case. **b,** Histogram over the number of registered forward contact tracing records per case, limited to contacts registered (residential address) in the city Düsseldorf. **c,** Histogram over the number of "forward contact tracing"-type edges per case in the Integrated Case Graph. **d,** Histogram over the number of registered incoming or outgoing forward contact tracing links per case in the directionalized ($t_d = 0$; see Methods) version of the Integrated Case Graph. **e,** Histograms over the number of "backward contact tracing"-type edges per case in the directionalized version of the Integrated Case Graph, stratified by direction of the edge.

Supplementary Figure 2: Forward contact tracing records over time. a, Shown is the monthly total number of registered SARS-CoV-2 cases registered and the proportion of cases with at least one attached forward contact tracing record (independent of whether the contact was mapped onto another case or not). **b,** Distribution over the number of forward contact tracing records per case, limited to cases with at least one attached contact tracing record and stratified by month of the year. **c,** Same data as in panel B., with a truncated y-axis focusing on the region between 1 and 10 forward contact tracing records.

Supplementary Figure 3: SARS-CoV-2 sequencing turnaround times. Distribution of SARS-CoV-2 sequencing turnaround times, measured from SARS-CoV-2 sample arrival at Heinrich Heine University to first availability of a resolved SARS-CoV-2 genome with <3000 unresolved (i.e. "N") characters on the dashboard of the Integrated Genomic Surveillance System Düsseldorf, tracked for a subset of n = 891 samples that were collected between April and June 2022. Samples that were not successfully sequenced to the desired level of SARS-CoV-2 genome completeness were not included.

Supplementary Figure 4: Data integration approach. Shown are the different steps of data integration leading to the Integrated Case Graph. Case, contact tracing and outbreak data were exported from the SurvNet database hosted at Düsseldorf Health Department and transferred into an intermediate MS Access application. SARS-CoV-2 samples were labeled with PCR test IDs and sampling dates; based on these, the first and last names and dates of births of the tested individuals could be obtained and merged with Düsseldorf Health Department case registration data. All case- or sample-identifying data (incl. names, dates of birth, sampling dates, address data) are hypothetical. In a final step, if a case was sequenced more than once, a unique sequence was selected. See Methods for details.

Supplementary Figure 5: SARS-CoV-2 variant distribution over time. Pango lineages [Rambaut et al. 2020] of the sequenced SARS-CoV-2 genomes, stratified by week.

Supplementary Figure 6: Distribution of genetic distances for contact tracing and "sameAddress"-type edges. Distribution of SARS-CoV-2 genetic distances for case pairs linked by different types of edges in the graph, stratified by edge type and only shown for case pairs for which a genetic distance could be calculated.

Supplementary Figure 7: Matched control dataset with scrambled contact tracing links. a, Difference between case registration dates for pairs of sequenced cases connected by real forward or backward contact tracing links and scrambled contact tracing edges. **b,** Number of contacts per case, comparing cases that are part of pairs of sequenced cases connected by real or scrambled contact tracing edges. **c,** Vaccination status of cases, comparing cases that are part of pairs of sequenced cases connected by real or scrambled contact tracing edges. **d,** Registration date of cases, comparing cases that are part of pairs of sequenced cases connected by real or

scrambled contact tracing edges. **e,** Genetic differences between cases, comparing cases that are part of pairs of sequenced cases connected by real or scrambled contact tracing edges.

Supplementary Figure 8: Contact tracing infection contexts, genetic evaluation and transmission rates. a, Genetic validation of infection contexts captured by forward tracing; shown is the number of case pairs that were connected by a forward contact tracing edge assigned to the corresponding putative context, stratified by whether the genetic distance genetic distance between the connected cases was ≤1 ("accepted") or >1 ("rejected"); edges for which no genetic distance was available were not included. **b,** Genetic validation of infection contexts captured by backward contact tracing; shown is the number of case pairs that were connected by a backward contact tracing edge assigned to the corresponding putative context; genetic validation analogous to panel A. **c,** Forward contact tracing contacts by context and associated putative context-specific transmission rates. Putative transmission rates were calculated for index cases registered until 17 December 2021.

Supplementary Figure 9: Context-specific distribution of genetic distances for contact tracing edges. Distribution of SARS-CoV-2 genetic distances for case pairs linked by forward (panel A) and backward (panel B) contact tracing edges in the graph, stratified by edge type and infection contexts, and only shown for case pairs for which a genetic distance could be calculated.

Supplementary Figure 10: CER genetic cluster sizes. a, Distributions of the size of genetic clusters computed for determining the CER, shown for genetic clustering thresholds $t_g = 0$ (left subpanel) and $t_g = 1$ (right subpanel). **b,** Mean sizes of genetic clusters computed for determining the CER, by month of the year and shown for genetic clustering thresholds $t_g = 0$ (left subpanel) and $t_g = 1$ (right subpanel). Clusters were assigned to months based on the average case registration date of the included cases. Error bars show 95% confidence intervals. Orange bars in the background show the total number of SARS-CoV-2 registered in Düsseldorf in the corresponding month.

Supplementary Figure 11: CER parameters and CER over time. a, Distribution of per-cluster CER values, shown for genetic clustering thresholds $t_g = 0$ (left subpanel) and $t_g = 1$ (right subpanel). **b,** CER by cluster size, for genetic clustering thresholds $t_g = 0$ (left subpanel) and $t_g = 1$ (right subpanel). Shown is the average of per-cluster CER values for all clusters of the specified size in cases, with error bars indicating 95% confidence intervals. **c,** CER by month, for genetic clustering thresholds $t_g = 0$ (left subpanel) and $t_g = 1$ (right subpanel). Shown is the average of per-cluster CER values for all clusters assigned to the specified month, with error bars indicating 95% confidence intervals; clusters were assigned to months based on the average case registration date of the included cases. All plots in all panels based on $t_d = -3$ and $t_j = 0$.

Supplementary Figure 12: Symptom onset and case registration dates. a, Difference between the case registration and symptom onset dates of individual cases. Cases with missing symptom onset data were excluded. **b,** Symptom onset date differences for pairs of sequenced cases with genetic distance ≤1 and connected by edges of type "backward contact tracing"; shown is the difference in symptom onset dates along the assumed directionality of infection as recorded during backward contact tracing (i.e., if case x specified case y as their putative infection source, the plot shows the symptom onset of x minus the symptom onset of y; if two cases specified each other as assumed infection sources, two date differences are included). All case pairs comprising cases with missing symptom onset data were excluded. **c,** Transmission directionality probability distribution, based on a simple Bayesian model. Assume there are two cases a and b; either a infected b or b infected a; define the observed data x as the difference in symptom onset date between a and b, i.e. $x = \text{symptom_onset}(a) - \text{symptom_onset}(b)$. The probability that b infected a conditional on the observed data is $P(b \to a|\text{x}) = \frac{\Pr(b\to a)\times \text{P}(\text{x}|b \to a)}{\Pr(b\to a)\times \text{P}(\text{x}|b \to a)+\Pr(a\to b)\times \text{P}(\text{x}|a \to b)}$. Assuming uniform priors, we obtain $P(b \to a|\text{x}) = \frac{\text{P}(\text{x}|b \to a)}{\text{P}(\text{x}|b \to a)+\text{P}(\text{x}|a \to b)}$. We empirically estimated a probability distribution $P_{Backward}$ on the difference in symptom onset dates between the infected case and the infecting case observed in backward contact tracing; specifically, $P_{Backward}(d) = \frac{|(c_1,c_2)\in E'_B:\text{symptom_onset}(c_2)-\text{symptom_onset}(c_1)=d|}{|E'_B|}$, where E'_B is the set of edges of type "backward contact tracing" in the Integrated Case Graph. We define $\text{P}(\text{x}|b \to a) = P_{Backward}(x)$. With respect to $\text{P}(\text{x}|a \to b)$, we note that x is, conditional on the assumption "$a \to b$" that a infected b, the difference in

symptom onset dates between the infecting case and the infected case, i.e., the opposite of the required parameterization for $P_{Backward}(d)$. To obtain the difference in symptom onset dates between the infected case and the infected case under the assumption that a infected b, x can be multiplied by -1; we thus obtain $\mathrm{P}(\mathrm{x}|b \rightarrow a) = P_{Backward}(-x)$. This gives $P(b \rightarrow a|\mathrm{x}) = \frac{P_{Backward}(x)}{P_{Backward}(x)+P_{Backward}(-x)}$. **D.** Expected numbers of directed edges with correct and incorrect directionality, stratified by whether they were retained or removed during graph directionalization (with parameter t_d set to 0 or 3) and shown separately for different thresholds on the genetic distance between the connected cases (no evaluation of genetic distances / $t_g = 0$ / $t_g = 1$). The probability that an edge (b, a) has the correct directionality was given by $P(b \rightarrow a|\mathrm{x})$ (see panel C.), with $P(b \rightarrow a|\mathrm{x})$ set to 0 for $x \leq -5$ and to 1 for $x \geq 5$.

Supplementary Figure 13: Integrated outbreak analysis, additional metrics. a, Outbreak sizes, stratified by outbreak type; outbreak size was defined as the number of cases assigned to the outbreak by Düsseldorf Health Authority. **b,** Outbreak durations, stratified by outbreak type; the duration of an outbreak was defined as the time in days from the earliest to the latest case registration date of the cases assigned to the outbreak. **c,** Forward contact tracing records per outbreak (defined as the cumulative number of forward contact tracing records of all outbreak-assigned cases, independent of whether the contacts were mapped onto other cases or not), stratified by outbreak type. **d,** "Forward contact tracing"-type edges connecting outbreak cases to non-outbreak cases in the Integrated Case Graph, per outbreak and stratified by outbreak type. **e,** Like panel D but normalized by outbreak size. **f,** "Forward contact tracing"-type edges connecting outbreak cases to non-outbreak cases in the Integrated Case Graph, per outbreak and stratified by outbreak type and by whether the connected non-outbreak case had a genetic distance of ≤1 to the outbreak ("accepted"), whether it had a genetic distance ≥2 ("rejected"), or whether a genetic distance could not be computed ("No distance available"). The genetic distance between a linked non-outbreak case and an outbreak was defined as the minimum genetic distance between the linked case and any case of the corresponding outbreak, and a distance could be computed if the outbreak contained at least one sequenced case and if the linked case was sequenced. **g,** Like panel F but normalized by outbreak size. **h,** "sameAddress"-type edges connecting outbreak cases to non-outbreak cases in the Integrated Case Graph, per outbreak and stratified by outbreak type. **i,** Like panel H but normalized by outbreak size. **j,** Like panel F but for "sameAddress"-type edges. **k,** Like panel G but for "sameAddress"-type edges. **l,** Number of genetically linked community cases, per outbreak and by outbreak type; genetically linked community cases were defined as cases not linked to the analyzed outbreak that had a genetic distance of 0 to at least one case of the corresponding outbreak. **m,** Like panel L but normalized by outbreak size.

Supplementary Figure 14: Manual investigation of outbreaks. Shown is an outbreak comprising 6 cases, 4 of which are sequenced and 2 of which are not. 2 cases were likely erroneously assigned to the outbreak (shaded in red), as indicated by PCR test dates in one case and genetic distances to other outbreak cases in the other case. Two cases are linked to the outbreak via contact tracing; one of these is, based on belonging to the same institutional context as the other outbreak cases, classified as a "missing" outbreak case (shaded in dark blue), and the other case is classified as an "outbreak-linked" case (shaded in light blue); the association between the cases and the outbreaks is supported by sequencing data in both instances. Three additional cases not assigned to the outbreak exhibit a genetic distance of 0 to at least one outbreak case. The first of the three cases is, based on belonging to the same institutional context as the other outbreak cases, classified as a "missing" outbreak case (shaded in dark green). For the second of the three cases, an epidemiological connection to the outbreak that is not present in the contact tracing data is discovered and the case is classified as outbreak-linked based on the discovered connection (shaded in medium-intensity green). Finally, for the third case (shaded in medium-intensity green), an epidemiological connection to the outbreak that involves a non-sequenced additional case (shaded light green) is discovered. The third case and the non-sequenced additional case are therefore classified as outbreak-linked; in the case of the non-sequenced additional case, its classification as outbreak-linked is based on the fact that it represents the only detected connection that can explain the genetic identity between the third sample and the outbreak.

Supplementary Figure 15: Subsampling of proportion of sequenced cases for the CER. a, Distribution of cluster sizes for different proportions of sequenced cases (x-axis) and $t_g = 0$ (left-hand panel) and $t_g = 1$ (right-hand panel). **b,** Absolute number of cases with a putative transmission source in the computed hypothetical

transmission chains, for different proportions of sequenced cases (x-axis) and based on clusters computed for $t_g = 0$ (left-hand panel) and $t_g = 1$ (right-hand panel). **c,** Cluster Explanation Rate (CER), for different proportions of sequenced cases (x-axis) and for $t_g = 0$ (left-hand panel) and $t_g = 1$ (right-hand panel). **d,** Proportion of cases with a putative infection source based on the assumption that all genetic links correspond to an epidemiolocal link, for different proportions of sequenced cases (x-axis) and $t_g = 0$ (left-hand panel) and $t_g = 1$ (right-hand panel).

Supplementary Figure 16: Subsampling of proportion of sequenced cases for characterization of large-scale transmission patterns. Left-hand panels: Average number of genetically linked cases (genetic distance 0 and difference in registration in dates ≤ 14 days) compared to the average number of sequenced cases linked via classical contact tracing for cases with contacts of the given category at different proportions of sequenced cases. Right-hand panels: Cases genetically linked to outbreaks and stratified by outbreak type and relative case registration date at different proportions of sequenced cases; 8 outbreaks that were associated with the Delta and Omicron variants and that overlapped, with their surrounding 2-week windows, with the expansion phases of these variants were not included.

Supplementary Figure 17: Overlap of "sameAddress"-type edges in the Integrated Case Graph with other edge types. a, Overlap with contact tracing edges. Shown is the overlap between edges of type "sameAddress", "forward contact tracing", and "backward contact tracing" in the Integrated Case Graph. **b, Overlap with "outbreak"-type edges.** For both panels, two edges of different types were counted as overlapping if they connected the same two cases. The label "Same Address - same Name" refers to edges of type "sameAddress-sameName"; the label "Same address", to edges of type "sameAddress-differentName".

Supplementary Figure 18: Size of "sameAddress"-type connected components. a, Distribution of the size of connected components in the Integrated Case Graph when only considering edges of type "sameAddress-sameName". **b,** Distribution of the size of connected components in the Integrated Case Graph when only considering edges of type "sameAddress-differentName".

Supplementary Figure 19: SARS-CoV-2 sample selection and assignment. a, Pairwise genetic distances between SARS-CoV-2 genomes assigned to the same case, prior to the selection of at most one viral genome sequencing record for all cases. The red line shows the mean of the distribution. **b,** Scatterplot comparing, for each generated SARS-CoV-2 genome after quality control and before outlier removal, the sampling date of the diagnostic swab used for SARS-CoV-2 sequencing (Y axis) to the Düsseldorf Health Authority registration date of the case that the viral genome sequencing record was assigned to (see Methods). The diagonal (difference = 0) is shown as a black line; red lines show the variance. Before proceeding to the selection of at most one unique viral genome per case, SARS-CoV-2 sequencing records which exhibited a difference between case registration and sample collection dates of < -21 or > 7 days were removed (see Methods).

Supplementary Figure 20: SARS-CoV-2 example transmission network. Transmission network of 8 cases, comprising 5 sequenced cases, 2 cases which were registered but not sequenced, and 1 undetected case. Red arrows show transmissions in the (generally unknown) complete transmission network; blue connections show 4 case connection paths (w_1 – w_4) between sequenced cases in the complete network, which connect the sequence pairs most closely related in terms of the unknown full network. A hypothetical transmission chain for the 5 sequenced cases may imply a putative infection source for up to 80% (4 / 5) of cases if "jump edges" (see Methods) are included and if case connection path w_4 can be found in the known epidemiological connections.

Supplementary Figure 21: Graph directionalization parameter t_d. The plots show, for two different values (0 and 3) of the "maximum symptom onset difference" directionalization parameter t_d ("Directionalization cut-off"), the number of edges in the Integrated Case Graph that were converted into one ("Directed edges") or two directed edges ("Undirected edges") in the directionalized version of the Integrated Case Graph, stratified by edge type (panel **a**) or by the genetic distance between the connected cases (panel **b**; only for case pairs consisting of two sequenced cases). Directionalization captures the concept of directionality of transmission and ensures that the symptom onset dates of cases connected in hypothetical transmission chains are compatible with the directionality of hypothetical transmission. In the process of directionalization, undirected edges of the form (c_1, c_2) are converted into either a single directed edge of the form (c_1, c_2) or (c_2, c_1), or into a pair of

directed edges of the form (c_1, c_2) and (c_2, c_1). Setting $t_d = 0$ implies that all connections (with the exception of links induced by backward contact tracing, see below) between two cases in the Integrated Case Graph become "directed" (i.e., are represented by a single directed edge) whenever there is any difference in symptom onset dates, and that all considered hypothetical transmissions always follow the direction of increasing symptom onset. The directionalization of edges of type "backward contact tracing" is carried out based on the individual cases' assessment of their assumed infection source; a "backward contact tracing" edge from case c_2 to case c_1 in the directionalized graph is created whenever c_1 specified c_2 as their assumed infection source, independent of symptom onset dates.

Supplementary Table Legends

Supplementary Table 1: Sequenced SARS-CoV-2 samples. The table includes, for each sequenced SARS-CoV-2 sample, a pseudonymized identifier ("Sample_ID"); the sample collection date; a binary indicator indicating whether the sequence was attached to a case node in the Integrated Case Graph; the number of undefined bases (Ns); GISAID, ENA and COGDAT upload identifiers; sample-to-sequence turnaround time (from arrival of sample at Heinrich Heine University to availability of the first viral genome sequence with <3000 "N" characters on the Integrated Genomic Surveillance System Düsseldorf website; not available for all samples); and Pango lineage classification results.

Supplementary Table 2: Total and sequenced cases per week. Total registered and sequences cases as well as case sequencing rate, by week.

Supplementary Table 3: Forward contact tracing contexts. For each forward contact tracing context, the table shows information on the number of recorded contacts, underlying index cases (the index case is the individual with whom the contact tracing interview was carried out), putative transmission events (i.e. edges in the Integrated Case Graph), putative transmission events with genetic distances available, (i.e. edges with a genetic distance), putative transmission events that were genetically validated (i.e. edges classified as "accepted"), and the corresponding putative transmission and genetic validation rates. For column "Number of putative transmission events", instances in which cases A and B specified each other as contacts during forward contact tracing contributed a count of 2; for column "Number of putative transmission events (unique edges in integrated graph)", such instances only contributed a count of 1 (as, prior to directionalization, edges in the Integrated Case Graph are undirected).

Supplementary Table 4: CER results. The table shows the results of the CER computation for the complete directionalized case graph G', i.e. summing over all genetic clusters. Shown are CER results for all combinations of parameter values controlling the CER computation process and for all permutations of edge types (indicated by an "X" in the corresponding edge type columns; i.e. the absence of an "X" indicates that the corresponding edge type was ignored when computing the CER). "Direction cutoff": Maximum symptom onset difference" parameter (t_d, "direction cutoff") multiplied by -1, determining which differences in dates of symptom onset were allowed between immediately linked cases in the constructed hypothetical transmission chains. "Clusters max distance": genetic clustering parameter (t_g). "Jump distance": "jump distance" parameter (t_j) that controled how many intermediate non-sequenced cases ("jump edges") any link between two cases in the constructed hypothetical transmission chains might comprise. "TrueSelbeAdresse": Edges of type "sameAddress-differentName". "SelbeAdresseNachname": Edges of type "SameAddressAndLastname". "SurvnetAngestecktBei": Backward contact tracing edges. "Outbreak": Edges of type "outbreak". "SurvnetKontaktperson": Forward contact tracing edges. "Jump edges count": Number of "jump edges" that represented intermediate non-sequenced cases available based on the specified parameterization (independently of whether these were used in the computed hypothetical transmission chains). "Used edges": Total number of edges in the hypothetical transmission chains computed for the specified parameterization. The four last columns show the number of "jump edges" used in the hypothetical transmission chains for the specified parameterization and the proportion of these edges relative to the total number of edges in these chains, stratified by how many intermediary non-sequenced cases the utilized edges comprised.

Supplementary Table 5: Hypothetical transmission chains context analysis. The table shows the number of edges contained in the computed hypothetical transmission chains, stratified by edge type and (when available)

further transmission context or outbreak type information. The columns "Forward" and "Backward" contain the number of forward and backward contact tracing edges for which no specific context was available. All computations based on $t_j = t_d = 0$. The row labeled "On cluster" shows results for hypothetical transmission chains that were computed incorporating genetic distances with $t_g = 0$; the row labeled "On entire graph ignoring sequences" shows results for hypothetical transmission chains that were computed based purely on epidemiological connections, i.e. ignoring genetic constraints.

Supplementary Table 6: Genetic clusters computed for determining the CER. List of genetic clusters. For each cluster, the table contains the ID of the cluster; the size of the cluster in cases; the time in days ("length") between the earliest and the latest case registration dates of the cases assigned to the cluster; the mean of the case registration dates of the cases assigned to the clusters; and the cluster-specific CER values, computed for the Cartesian product of $t_j \in$ Fehler! Textmarke nicht definiert. and $t_d \in \{0,1\}$. The prefix of the cluster ID indicates whether the specified cluster is part of the cluster set computed using a genetic similarity threshold t_g of 0 or 1.

Supplementary Table 7: Outbreak analysis results for individual outbreaks. With the exception of one additional column specifying the month in which the earliest case of each outbreak was registered, all included columns are also found in Supplementary Table 8 and the definitions given in Supplementary Table 10 apply (with the modification that no agglomeration by outbreak type is carried out for any of the metrics; in this table, each outbreak is – when applying the definitions given in Supplementary Table 10 – effectively treated as a separate category).

Supplementary Table 8: Outbreak analysis results agglomerated by outbreak type. See Supplementary Table 10 for a detailed legend of the included fields.

Supplementary Table 9: Identified links between the outbreaks. The table shows, for all pairs of outbreaks, whether a link between the two outbreaks was identified. For each linked pair of outbreaks, the table specifies the number of epidemiological links between the two outbreaks (i.e. of edges connecting any case from the one outbreak to any case of the other outbreak in the Integrated Case Graph) and which types of edges these were induced by ("Forward", "Backward," "SameAddress"); the number of genetically linked cases (i.e. the number of unordered pairs of sequenced cases from both outbreaks with a genetic distance of 0; "Genetically linked"); and whether the link was confirmed manually ("Manual analysis", encoded as a binary true/false variable).

Supplementary Table 10: Outbreak analysis results column legend. Definition of fields in Supplementary Table 7. The given definitions also apply to Supplementary Table 8, with the modification that no agglomeration by outbreak type is carried out in Supplementary Table 8; i.e. in table Supplementary Table 8, each outbreak is – according to the definitions given for Supplementary Table 7 – effectively treated as its own category.

Supplementary Table 11: Controlled forward contact tracing context vocabulary. Vocabulary terms used for recording forward contact tracing infection contexts, in their German original and English translation.

Methods

Implementation of genomics-enhanced contact tracing in Düsseldorf

Genomics-enhanced contact tracing was implemented using the Integrated Genomic Surveillance System Düsseldorf (IGSD), which has been fully described elsewhere [Houwaart et al. 2022, Walker et al. 2022]. Briefly, the high-level aims of the IGSD were to monitor viral evolution in the Düsseldorf area and to investigate whether a combination of high-density genomic surveillance with classical epidemiological approaches could enable an improved understanding of SARS-CoV-2 transmission in the population at large. The IGSD was implemented as a collaboration between Heinrich Heine University Düsseldorf (HHU), Zotz | Klimas (ZK) and Medizinische Laboratorien Düsseldorf (MLD), two large commercial diagnostic laboratories from Düsseldorf, and Düsseldorf Health Authority. Viral samples provided by ZK and MLD, as well as viral samples collected from patients treated at Düsseldorf

University Hospital, were rapidly Nanopore-sequenced using HHU's SARS-CoV-2 sequencing platform; SARS-CoV-2 sequences generated by MLD were also integrated.

Case registration and contact tracing carried out by Düsseldorf Health Authority

SARS-CoV-2 case data collection and contact tracing, using the SurvNet application [Faensen et al. 2006, Krause et al. 2007] for data storage and management, were carried out by Düsseldorf Health Authority under the mandate of the Law on the Prevention of Infection (Infektionsschutzgesetz (IfSG) based on the classification of SARS-CoV-2 as a notifiable pathogen in Germany since 2020. This involved (i) the reporting to Düsseldorf Health Authority of all Düsseldorf residents tested positive for SARS-CoV-2 by diagnostic laboratories; (ii) the registration of the personal data of all registered cases by Düsseldorf Health Authority; (iii) contact tracing interviews with all Düsseldorf cases conducted by Düsseldorf Health Authority, the participation in which was mandatory; (iv) the reporting of all suspected outbreaks (see "Retrospective investigation of outbreaks" for the applied definition of an outbreak) and their involved cases to Düsseldorf Health Authority. Contact tracing was based on the official contact tracing guidelines in place at the respective time, as published by the Robert-Koch-Institute. It always involved a forward contact tracing component and also typically a backward contact tracing component. Forward contact tracing was carried out for quarantine and isolation purposes, aiming at the identification of all individuals that a case had been in contact with around a time window of 2 days before symptoms onset (if symptomatic) or 2 days before the case's positive diagnostic test (if asymptomatic), irrespective of the potential directionality of transmission. Personal data of unvaccinated contacts, and of vaccinated contacts registered up until 20 April 2021, were always entered into SurvNet in a structured manner (and thus represented as edges in the Integrated Case Graph, see below); on 21 April 2021, mandatory quarantine requirements were lifted for fully vaccinated contacts, and whether and in which form (structured or using free-text entry fields) personal data of fully vaccinated contacts were entered into SurvNet after that date was decided by the individual carrying out the contact tracing interview. Of note, the number of registered contacts per case remained relatively similar over the course of 2021, except for November and December 2021 (Supplementary Fig. 5). During backward contact tracing, the infected individual was asked whether they could identify whom they thought they had likely acquired their infection from. Backward contact tracing data were usually entered into SurvNet in a structured manner. During contact tracing interviews, responses by the interviewed individuals were assessed for plausibility and likelihood that the contact led to a transmission; contacts that were deemed unlikely to have led to a transmission (e.g., between two masked individuals in a well-ventilated area) were not recorded. Contact tracing also involved an assessment of the context in which the detected contacts had taken place in; for structured forward contact tracing records, context information was stored in a structured manner as part of the contact tracing records using a controlled vocabulary (Supplementary Table 11); otherwise, context information was sometimes stored in free-text entry fields.

Genetic distance matrix

A matrix of genetic distances between all analyzed sequences was calculated as previously defined [Houwaart et al. 2022]. Briefly, based on a multiple sequence alignment (MSA) of the included sequences computed using MAFFT [Katoh and Standley 2013] following GISAID [Shu and McCauley 2017] instructions, the distance $d(x, y)$ between samples x and y was defined as the count of differences between the entries of x and y in the MSA, (i) ignoring leading or trailing "gap" characters, (ii) accounting for International Union of Pure and Applied Chemistry (IUPAC) ambiguity codes, (iii) treating subsequent non-matching gaps columns as a single difference, (iv) ignoring deletions in the MSA entry of x aligned to 'N' characters in y and vice versa, and (v) not counting any differences found

between the beginning of the MSA and the 20th A/C/G/T character of either sequence and the end of the MSA and the 20 last A/C/G/T characters of either sequence.

Integrating genomic and viral genome sequencing data into a case graph

Integration of genomic, case, and contact tracing data was carried out using a custom Microsoft Access database application deployed within the protected IT infrastructure of Düsseldorf Health Authority. All personally identifiable information remained at Düsseldorf Health Authority. See Supplementary Fig. 2 for a schematic of the data integration process.

As a first step, case and contact tracing data for SARS-CoV-2 cases from Düsseldorf were exported from the SurvNet application and imported into the custom Access database. Routinely collected data included (a) case-identifying information, such as name, date of birth and registered address; (b) forward contact tracing data; forward contact tracing data comprised the SurvNet database ID of the corresponding case (i.e. specifying the individual with whom the contact tracing interview was carried out), as well as the first and last names, the date of birth, and the residential status (Düsseldorf resident or not) of the registered contacts; the exported forward contact tracing data records, however, did not comprise information on the subsequent infection or case registration status of the contacts (see next section); (c) backward contact tracing data ("InfectedBy" field), only available for a small proportion of cases; backward contact tracing records comprised the SurvNet case ID of the individual with whom the contact tracing interview was carried out (the infected individual) as well as the SurvNet case ID of the individual who was registered as the putative source of the infection (i.e. both individuals were necessarily registered as cases); (d) outbreak data, specifying, for each registered outbreak, details on the specific institutional context as well as a list of case IDs assigned to the outbreak.

As a second step, the following post-processing steps were carried out. (i) The total number of registered forward contact tracing records on a per-case basis was tabulated and attached to each case record, separately for all registered contacts and registered contacts from Düsseldorf. (ii) For each registered forward contact tracing contact from Düsseldorf, the case database was queried for cases with matching first and last names and a matching date of birth; for each match, a case-resolved forward contact tracing record, comprising the case IDs of both the interviewed individual and of the registered contact, as well as the database ID(s) of the contact tracing record(s), was created and stored in the database (with additional filters on the maximum difference between the registration dates of any two cases so-connected applied later, see below; these date-based filtering steps also resolved instances in which a contact tracing record matched more than one case record, e.g. because the same individual tested SARS-CoV-2-positive more than once); (iii) For each case ("query case"), other cases with case registration dates within a 30-day window around the registration date of the query case (≤ 30 days absolute date difference) and (a) with the same registered address as the query case or (b) sharing the same registered address and the same last name as the query case were identified and stored as "SameAddress" and "SameAddressAndLastname" records, comprising the case IDs of the linked cases, in the database. (iv) For each outbreak, the set of all pairs of cases assigned to the outbreak was determined and each pair was stored as a record of type "SameOutbreak", comprising the case IDs of the two member cases.

As a third step, SARS-CoV-2 genome sequencing records were matched with cases, based on the following procedure. (i) All sequenced samples, and therefore all sequenced SARS-CoV-2 genomes, were labelled with a sample collection date and a PCR test ID by the diagnostic laboratory providing the sample. (ii) Based on these data, we queried data sheets provided by the diagnostic laboratories for the first and last name and the date of birth of the individuals that had provided the sequenced

sample. (iii) We matched these data against the SurvNet case registration records; if exactly one match covering all 3 criteria was identified, the viral genome sequence was attached to the SurvNet case record; otherwise, manual curation was carried out to account e.g. for last name spelling mistakes in one of the two data sources. (iv) For all viral genome sequences attached to case records, the difference between case registration date and sample collection date was calculated, and all n = 36 viral genome sequences with a difference < -21 or > 7 were removed (Supplementary Figure 19)

As a fourth step, for all n = 533 cases c with more than one assigned viral genome sequencing record, a unique record was selected based on the following procedure. (i) If all sequences attached to a case had genetic distance ≤1 between each other, we selected the sequence with the smallest number of undefined nucleotides ("N" characters). (ii) Otherwise, define the set $C_{Contacts-Sequenced}$ as the set of other cases that were linked to case c via contact tracing and that had attached viral genome sequencing data (there we no instances of cases in $C_{Contacts-Sequenced}$ that had more than one attached viral genome sequencing record). (iii) For each viral genome sequencing record s attached to c (more than one by definition), define $compatible(c, s)$ as the set of cases in $C_{Contacts-Sequenced}$ that had an associated viral genome sequencing record with genetic distance $\leq$ 1 to s (see Supplementary Figure 19). (iv) Determine $\arg\max_{s} compatible(c, s)$ and attach the corresponding viral genome sequencing record s to c.

Finally, the integrated dataset was exported as an Integrated Case Graph in which (a) each registered case from Düsseldorf, together with non-identifiable metadata such as the number of total forward contact tracing contacts and forward contact tracing contacts from Düsseldorf, was represented as a node; (b) connections between pairs of cases, i.e. forward and backward contact tracing relationships, "sameAddress"-type information, as well assignment of two cases to the same outbreak, were represented as undirected edges; and (c) SARS-CoV-2 genome sequencing records of cases were attached to nodes in the case graph. Edges of type "sameAddress-sameName" were created based on records of type "SameAddressAndLastname"; edges of type "sameAddress-differentName" were created for all sample pairs that appeared in "SameAddress"-type records, but not in "SameAddressAndLastname"-type records. All edges (c_1, c_2) of type "backward contact tracing" between cases c_1 and c_2 were annotated with the information on whether c_1 specified c_2, and c_2, c_1, as their assumed infection sources (note that these two cases were not mutually exclusive). All edges between pairs of cases with an absolute difference in case registration dates of more than 14 days were removed [Ryu et al. 2022]. A distance matrix for all SARS-CoV-2 genomes attached to the nodes of the graph was exported with the graph.

Infection context analysis

To characterize context-specific transmission probabilities, we carried out a separate database export of all forward contact tracing records stored in SurvNet, comprising, for all exported records, the SurvNet database ID of the index case (i.e. specifying the individual with whom the contact tracing interview was carried out); the residential status (Düsseldorf resident or not) of the contact; the database ID of the contact tracing record; and the contact context (determined by Düsseldorf Health Authority staff during contact tracing; see Supplementary Table 11). We filtered the exported records for index cases with a case registration date ≤ 17 December 2021 and represented in the Integrated Case Graph and removed all records with contacts not registered at a Düsseldorf address. A recorded contact was classified as associated with a potential transmission event if and only if (i) a matching case-resolved forward contact tracing record (see previous section; matching was carried out based on the case ID of the index case and the database ID of the contact tracing record) was identified and (ii) the identified case-resolved forward contact tracing record was represented by an edge of type

"forward contact tracing" in the Integrated Case Graph after application of all filtering steps; in all instances satisfying the two conditions, the individual that the contact was registered with had also tested SARS-CoV-2 positive in a period of 14 days around the registration date of the index case, compatible with a direct transmission event. Context-specific transmission probabilities were then calculated by dividing the number of contacts associated with a potential transmission event by the total number of registered contacts for each context. Context annotation for edges of type “forward contact tracing” was carried out based on the same database export and matching process, but omitting the date filtering step (i.e., the annotation process was also applied to edges associated with index cases registered after 17 December).

For backward contact tracing records, export of infection context information from SurvNet in a structured manner was not possible. We therefore employed a manual classification approach, based on review of the data stored in SurvNet (involving all structured case data as well as free-text notes taken during routine contact tracing interview, if available). Each backward contact tracing contact was, based on the definitions given below, assigned to one of the following categories: (i) “Private household”: Contact between two individuals in the context of a private household, involving at least one overnight stay; (ii) “Recreational activity”: Contact associated with a recreational activity, such as taking a walk, attending a family party, visiting a friend’s place (without an associated overnight stay), or contact during participation in a shared hobby (e.g. football); (iii) “School”: Contact in the context of a primary or secondary school, including contacts between students and teachers; (iv) “Kindergarten/Daycare”: Contact in the context of a kindergarten or daycare nursery (German “KiTa”), including contacts between children and daycare personnel; (v) “Workplace”: The involved individuals interacted in a work context; (vi) “Asylum/homeless care home”: The individuals had overlapping stays at a care home for asylum seekers or homeless individuals; (vii) “Elderly care home”: Contact in the context of a care home for the elderly, including contacts between care home personnel and inhabitants; (viii) “Hospital”: Contact in the context of a hospital, including contacts between patients and staff; (ix) “Assisted living care home”: Contact in the context of a care home for assisted living for non-elderly individuals (German “betreutes Wohnen”), including contacts between inhabitants and staff.

Generation of a scrambled-edges control dataset for analysis of contact tracing genetic distances

To investigate whether genetic distances observed for case pairs connected by contact tracing edges may be the result of incidental genetic similarity of cases sequenced at approximately the same time, we generated a matched control dataset with randomized connections between sequenced cases registered at approximately the same time; the genetic distances along the randomized edges could then be compared to the genetic distances observed for real contact tracing edges. To generate the randomized dataset, we applied the following procedure. We identified all 3,862 cases that were sequenced and that either had a forward or backward contact tracing edge in the Integrated Case Graph. We created candidate randomized case pairs by first generating all 14,915,044 possible ordered case pairs from the identified 3,862 cases and removed all pairs that exhibited a registration date difference of more than 14 days. Furthermore, we removed all pairs that were connected by real forward or backward contact tracing links in the Integrated Case Graph, as well as all pairs linking a case to itself and case pairs (a, b) for which forward or backward contact tracing edges (a, x) and (b, x) – where x denotes a joint shared contact of a and b – existed. From the set of remaining 1,616,999 candidate randomized case pairs, we selected the 1,011 pairs that exhibited the highest degree of similarity (see Supplementary Fig. 9) to the 1,011 real case pairs connected by edges of type “forward contact tracing” or “backward contact tracing” (and with a genetic distance available) in the

Integrated Case Graph, taking into account i) vaccination status, ii) date of index case registration, iii) mean case registration date, iv) distance between the case registration dates, v) number of registered contacts. The matching procedure was implemented using a custom R script and R packages "lubridate", "stringr" and "data.table".

Retrospective investigation of outbreaks

For all outbreaks recorded by Düsseldorf Health Authority, routinely collected outbreak data, including the type of institution, the involved cases and the duration of the outbreak, were extracted from the database of Düsseldorf Heath Department and combined with the data represented in the Integrated Case Graph for analysis. An outbreak was defined as "not genetically homogeneous" if a graph defined by (i) the sequenced outbreak cases as nodes and (ii) inter-case genetic distances as edges contained, after removal of edges corresponding to genetic distances > 1, more than one connected component; an individual case was classified as erroneously assigned to the outbreak if it was not part of the largest connected component of the graph so-defined (i.e., all genetically homogeneous outbreaks contained no erroneously assigned cases according to this definition). A community case (here defined as a case not part of any other outbreak of the same category as the outbreak under investigation) was defined as connected to an outbreak if it was connected to any case of the considered outbreak in the Integrated Case Graph; for outbreaks with ≥ 1 sequenced cases and all outbreak-linked sequenced community cases, the corresponding links were classified as "sequencing-confirmed" if the genetic distance between the linked community case and any sequenced outbreak case was $\leq$ 1. For outbreaks with ≥ 1 sequenced case, we also identified community cases that were only linked to the outbreak on a genetic basis, i.e. independent of epidemiological information; for this analysis, genetically linked community cases were defined as community cases that exhibited a genetic distance of 0, and that had a case registration date difference to any outbreak case of $\leq$ 14 days. Two outbreaks A and B were classified as epidemiologically linked if any case of outbreak A was linked to any case of outbreak B in the Integrated Case Graph; two outbreaks A and B were classified as genetically linked if any sequenced case of outbreak A had a genetic distance $\leq$ 1 to any sequenced case of outbreak B.

For school outbreaks, an in-depth analysis was carried out (Supplementary Figure 14), comprising the following steps and based on the definition of an outbreak as a group of cases connected by suspected or confirmed transmission events in a shared defined (typically institutional) context. First, epidemiological identification of cases falsely assigned to the outbreak: An evaluation of all available test and symptom onset dates for all outbreak cases was carried out and cases for which the available test and symptom onset data were not compatible with the other outbreak cases were identified. Second, identification of missing cases based on contact tracing and genetic data: For each outbreak with ≥ 1 sequenced case, we identified all cases that (i) were linked to at least one outbreak case by structured forward contact tracing data; (ii) were not already assigned to the outbreak; (iii) exhibited a genetic distance of 0 to at least one case in the outbreak; (iv) belonged, based on the available case data, to the same (typically institutional) context as the outbreak (e.g., were students or teachers at the school at which the outbreak had taken place). Third, analysis of non-structured and backward contact tracing data: For a subset of outbreaks (identified by column "Analysis of non-structured contact information" in table Supplementary Table 7), contact tracing information entered in a non-structured manner into the SurvNet application (i.e., using free-text entry fields) as well as backward contact tracing data were also analyzed during the previous step. Fourth, genetically driven identification of missing or linked cases: For a subset of outbreaks with ≥ 1 sequenced case (identified by column "Outbreak-external links investigated based on individual case genetic distance checks" in table Supplementary Table 7), we identified cases that (i) were not already linked to the outbreak by either direct assignment to the outbreak or via any contact tracing data; (ii) exhibited a genetic

distance of ≤ 1 and a PCR test date difference of ≤ 4 weeks to at least one outbreak case; (iii) met one of the following three criteria of linkage to the outbreak: "missing outbreak case", defined as belonging to the (institutional) context of the outbreak; "direct epidemiological linkage", defined as a direct epidemiological link (e.g. shared household, family connection, workplace) to at least one outbreak case; "indirect epidemiological linkage", defined as a direct epidemiological link to another case X with a direct epidemiological link to at least one outbreak case. For connections of the latter (indirect epidemiological) type, we furthermore required that "X" was either non-sequenced or that its viral genome was compatible (distance ≤ 1) to the outbreak; if "X" was not sequenced and found to represent the only connection between a sequenced case classified as "indirectly epidemiologically linked" and the outbreak, "X" was classified as an outbreak-linked case with indirect genetic support and further classified into a missing outbreak case or a linked community sample. Fifth, assessment of potential outbreak-associated transmission chains: We carried out a comprehensive manual assessment and analysis of potential infection chains associated with the investigated outbreaks. This led, for example, to the conclusion that the only sequenced case of outbreak CVD-DÜS-SCHULE-2021-0182 was likely a mis-assigned (see Supplementary Note 1). Sixth, identification of related outbreaks: Two outbreaks were classified as related if there was, according to the criteria defined above, at least one case from the one outbreak that exhibited direct or indirect genetic linkage to at least one case from the other outbreak and if the connection between the two outbreaks was also supported by a direct or indirect epidemiological connection between at least one case from the one outbreak to at least one case from the other outbreak.

Cluster Explanation Rate

Given a single cluster C of N genetically related cases, and a set of epidemiological connections between them, the Cluster Explanation Rate (CER) measures the proportion of cases in the cluster that a putative infection source can be identified for based on a hypothetical transmission chain constructed from the epidemiological connections for the cases in the cluster. When generalized to multiple clusters, the CER is computed by summing over the number of cases with a putative infection source and the total number of cases across the considered clusters. Finally, at the level of a complete dataset, the CER is determined by first clustering all sequenced cases by genetic similarity and then computing the CER of the clusters so-determined; at this level, the CER provides a measure of how well the collected epidemiological data explain overall observed genetic similarities.

Formally, let $G' = (V, E')$ be a directionalized and augmented version of the case graph $G = (V, E)$; directionalization and augmentation are required for ensuring that hypothetical transmission chains considered for computing the CER are consistent with respect to symptom and/or case registration dates and for including hypothetical transmission chains that involve intermediate non-sequenced cases (see below). All CER computations are based on G'. We first define the CER of a single cluster C, i.e. of a subset of nodes of the case graph G', of genetically related cases; let t_g denote the genetic distance threshold that was used for the clustering (defined in detail below). Let the set $E'(C)$ represent the set of genetically supported epidemiological connections between the cases in C; $E'(C)$ is defined as the subset of directed edges between C in G' that connect two cases with a pairwise genetic distance $\leq t_g$. A hypothetical transmission chain h is defined as an acyclic subset of $E'(C)$ such that no node $c \epsilon C$ has more than one incoming edge from the set h (note that the definition allows for partial transmission chains that do not connect all nodes; epidemiologically, such transmission chains may be interpreted to include cases outside of the cluster C; Supplementary Figure 20; in addition, no constraints are placed on the number of outgoing edges, i.e. the set of considered transmission chains includes "branching" transmission chains or "networks"). The CER for cluster C in case graph G' is then defined as

$$\mathrm{CER}_{G'}(C) := \frac{\max_{h \in H(C)} |h|}{|C|},$$

, where $H(C)$ is the set of all possible hypothetical transmission chains for the cases in cluster C and their epidemiological connections $E'(C)$; $|h|$ is the size of the hypothetical transmission chain h in edges; $|C|$ is the number of cases in C; and $\max_{h \in H} |h|$ is computed according to the heuristic algorithm defined below.

For a set W of multiple clusters of genetically related cases in case graph G', we define the CER as

$$\mathrm{CER}_{G'}(W) := \frac{\sum_{C \in W}\left(\max_{h \in H(C)} |h|\right)}{\sum_{C \in W}(|C|)}.$$

Finally, to define the CER for a case graph G', the sequenced cases in G' are clustered into groups of genetically related isolates, based on a similarity threshold t_g. To do so, we consider a graph that consists of the sequenced cases in G' as nodes and that includes all pairwise genetic distances as undirected edges; we remove all edges corresponding to genetic distances $> t_g$; and, finally, we define the set $\mathrm{genetic_clusters}(G')$ as the set of remaining connected components with size > 1 in the graph. Any two cases c_1 and c_2 from the same cluster either have genetic similarity $\leq t_g$ or they are connected by a path of sequenced cases with intermediate pairwise distances between $\leq t_g$; furthermore, the computed clusters are non-overlapping. Based on the computed clusters, we define the CER for a case graph G' as

$$\mathrm{CER}(G') = \mathrm{CER}_{G'}\big(\mathrm{genetic_clusters}(G')\big).$$

Directionalization, yielding a directed case graph $G' = (V, E')$, enables the definition of hypothetical transmission chains at the level of a directed graph between cases, capturing the concept of directionality of transmission and ensuring that all considered pairwise links between cases are consistent with respect to symptom onset (or, if unavailable, case registration) dates. In G', a directed edge (c_1, c_2) represents a possible hypothetical transmission event from c_1 to c_2. Directionalization is followed by potential augmentation of the graph with "jump edges", representing links in hypothetical transmission chains between sequenced cases that involve intermediate non-sequenced cases. For directionalization, E' is constructed by including, for each (undirected) edge $e = (c_1, c_2) \in E$, one or two directed edges, as defined below. For all edges except for edges of type "backward contact tracing", directionalization is controlled by the parameter t_d, specifying the allowed difference in symptom onset dates in days between linked cases (according to the definition below). Denote the date of symptom onset of case c as $s(c)$; if the symptom onset date for case c is unavailable, $s(c)$ is set to the case registration date of c minus 3 days, based on an empirical analysis of the difference between symptom onset and case registration dates for samples for which both dates are available (Supplementary Fig. 23). We distinguish between the following cases: (i) if $\mathrm{abs}(s(c_1) - s(c_2)) \leq t_d$, edges (c_1, c_2) and (c_2, c_1) are added to E'; (ii) if $s(c_1) - s(c_2) > t_d$, edge (c_2, c_1) is added to E'; (iii) otherwise, $s(c_2) - s(c_1) > t_d$ is true, and edge (c_1, c_2) is added to E'. Note that these definitions imply that one undirected edge in the original case graph may be represented by two directed edges in the directed case graph, if the observed symptom onset dates are consistent with transmission in both directions, depending on the threshold t_d. For undirected edges (c_1, c_2) of type "backward contact tracing" in the original case graph G, a directed edge from c_1 to c_2 is added to E' if case c_2 specified case c_1 as their assumed infection source during infection source during backward contact tracing; and a directed edge from c_2 to c_1 is added to E' if case c_1 specified case c_2 as their assumed infection source during backward contact tracing. For augmentation with "jump distance" parameter $t_j = 0$, no additional edges are added to G'. For augmentation with $t_j = 1$, an edge from c_1 to c_2 is

added to E' for all instances of the form (c_1, a, c_2), in which (i) c_1 and c_2 represent two sequenced cases; (ii) a represents a non-sequenced case; (iii) there are no edges directly connecting c_1 to c_2; (iv) there is at least one edge from c_1 to a; (v) there is at least one edge from a to c_2; (v) the genetic distance between c_1 to c_2 is $\leq (t_j + 1) * t_g$. Augmentation for $t_j = 2$ proceeds analogously for instances of the form (c_1, a, b, c_2).

The computed $\mathrm{CER}(G')$ depends on the parameter used for the genetic clustering (t_g), the "maximum symptom onset difference" parameter used for directionalization (t_d), and the "jump distance" parameter (t_j). To assess the impact of different parameter choices on the computed CER, all CER computations are carried out for all combinations (i.e., the outer product) of the parameter values $t_g = \{0,1\}$, $t_d = \{0,3\}$ and $t_j = \{0,1,2\}$. For t_d, a value of 0 implies constraining the direction of hypothetical transmission whenever there is any difference in symptom onset dates (i.e., a conservative choice); -3 was chosen empirically based on inspection of observed symptom onset dates for sample pairs connected by edges of type "backward contact tracing", which are intrinsically directed (Supplementary Fig. 23). Directionalization results for different edge types and the two employed thresholds are visualized in Supplementary Figure 21.

$\max_{h \in H(C)} |h|$ for a cluster C is computed according to the following procedure. Initialize the variable h' as the empty set; h' is populated progressively with edges from $E'(C)$, and, after termination, the set h' represents a heuristic approximation of $\arg\max_{h \in H(C)} |h|$.

The following steps are carried out until termination. First, define M as the set of nodes $c \in C$ that are neither the origin nor the destination of any of the edges currently in h'. Second, for each $c \in M$, define $\mathrm{reachable}(c)$ as the set of other nodes in M that can be reached from c, employing paths that consist of the directed edges $E'(C)$ and that only involve intermediate nodes that are also part of M. $\mathrm{reachable}(c)$ can be computed using a depth-first search. Third, find $c_{max} = \arg\max_{c \in M} |\mathrm{reachable}(c)|$ by iterating through the current members of M. If $|\mathrm{reachable}(c_{max})| = 0$, terminate; otherwise, let B be the set of edges underlying the paths connecting c_{max} to $\mathrm{reachable}(c)$. If necessary, remove edges from B so that B does not contain any cycles and so that there is no node in $\mathrm{reachable}(c)$ with more than one incoming edge from B. Finally, add the edges in B to h' and go back to the first step.

Ethics statement

This study was approved by the ethics committee of the Medical Faculty of Heinrich Heine University Düsseldorf (#2020–839).

Funding

We acknowledge funding by the Ministry for Work, Health and Social Affairs of the State of North Rhine-Westphalia ("24.04.01 Gen. u. IKA" and CPS-1-1A); the German Federal Ministry of Education and Research (Bundesministerium für Bildung und Forschung; Netzwerk Universitätsmedizin, GenSurv/MolTraX), award number 01KX2021; by the Jürgen Manchot Foundation; and by the Deutsche Forschungsgemeinschaft (DFG) award 428994620.

No competing interests

All authors have completed the ICMJE uniform disclosure form and declare: no support from any organization for the submitted work; no financial relationships with any organizations that might have an interest in the submitted work in the previous three years; no other relationships or activities that could appear to have influenced the submitted work.

Acknowledgements

We thank Gil McVean and Marc Janssen for helpful discussions. We also thank the contact tracing team of Düsseldorf Health Authority for their commitment and the countless extra hours.

References

Allen, K., A. Marmor and D. Pourmarzi (2022). "Pens down: An outbreak of the B.1.617.2 SARS-CoV-2 variant in an Australian high school, August 2021." Commun Dis Intell (2018) **46**.

Andersen, K. G., B. J. Shapiro, C. B. Matranga, R. Sealfon, A. E. Lin, L. M. Moses, O. A. Folarin, A. Goba, I. Odia, P. E. Ehiane, M. Momoh, E. M. England, S. Winnicki, L. M. Branco, S. K. Gire, E. Phelan, R. Tariyal, R. Tewhey, O. Omoniwa, M. Fullah, R. Fonnie, M. Fonnie, L. Kanneh, S. Jalloh, M. Gbakie, S. Saffa, K. Karbo, A. D. Gladden, J. Qu, M. Stremlau, M. Nekoui, H. K. Finucane, S. Tabrizi, J. J. Vitti, B. Birren, M. Fitzgerald, C. McCowan, A. Ireland, A. M. Berlin, J. Bochicchio, B. Tazon-Vega, N. J. Lennon, E. M. Ryan, Z. Bjornson, D. A. Milner, Jr., A. K. Lukens, N. Broodie, M. Rowland, M. Heinrich, M. Akdag, J. S. Schieffelin, D. Levy, H. Akpan, D. G. Bausch, K. Rubins, J. B. McCormick, E. S. Lander, S. Gunther, L. Hensley, S. Okogbenin, C. Viral Hemorrhagic Fever, S. F. Schaffner, P. O. Okokhere, S. H. Khan, D. S. Grant, G. O. Akpede, D. A. Asogun, A. Gnirke, J. Z. Levin, C. T. Happi, R. F. Garry and P. C. Sabeti (2015). "Clinical Sequencing Uncovers Origins and Evolution of Lassa Virus." Cell **162**(4): 738-750.

Bludau, A., A. Jack, N. Fischer, J. Dreesman, C. Drosten, R. Egelkamp, L. Ehlkes, F. Feil, A. Grundhoff, H. Grundmann, P. Kreuzer, M. Monazahian, I. Overesch, D. Schmitt, M. Troger, A. von Reiswitz, J. Weber, A. Dilthey, C. Hornberg, S. Reuter and S. Scheithauer (2025). "Use of integrated genomic surveillance by local public health authorities: Recommendations based on a mixed-methods study of current adoption, applications and success factors, Germany, 2023." Euro Surveill **30**(13).

COVID-19 Genomics UK (COG-UK) (2020). "An integrated national scale SARS-CoV-2 genomic surveillance network." Lancet Microbe **1**(3): e99-e100.

Faensen, D., H. Claus, J. Benzler, A. Ammon, T. Pfoch, T. Breuer and G. Krause (2006). "SurvNet@RKI--a multistate electronic reporting system for communicable diseases." Euro Surveill **11**(4): 100-103.

Faria, N. R., E. C. Sabino, M. R. Nunes, L. C. Alcantara, N. J. Loman and O. G. Pybus (2016). "Mobile real-time surveillance of Zika virus in Brazil." Genome Med **8**(1): 97.

Ferretti, L., C. Wymant, J. Petrie, D. Tsallis, M. Kendall, A. Ledda, F. Di Lauro, A. Fowler, A. Di Francia, J. Panovska-Griffiths, L. Abeler-Dorner, M. Charalambides, M. Briers and C. Fraser (2024). "Digital measurement of SARS-CoV-2 transmission risk from 7 million contacts." Nature **626**(7997): 145-150.

Garcia-Bernardo, J., C. Hedde-von Westernhagen, T. Emery and A. J. van Hoek (2024). "Assessing COVID-19 transmission through school and family networks using population-level registry data from the Netherlands." Sci Rep **14**(1): 31248.

Gudbjartsson, D. F., A. Helgason, H. Jonsson, O. T. Magnusson, P. Melsted, G. L. Norddahl, J. Saemundsdottir, A. Sigurdsson, P. Sulem, A. B. Agustsdottir, B. Eiriksdottir, R. Fridriksdottir, E. E. Gardarsdottir, G. Georgsson, O. S. Gretarsdottir, K. R. Gudmundsson, T. R. Gunnarsdottir, A. Gylfason, H. Holm, B. O. Jensson, A. Jonasdottir, F. Jonsson, K. S. Josefsdottir, T. Kristjansson, D. N. Magnusdottir, L. le Roux, G. Sigmundsdottir, G. Sveinbjornsson, K. E. Sveinsdottir, M. Sveinsdottir, E. A. Thorarensen, B. Thorbjornsson, A. Love, G. Masson, I. Jonsdottir, A. D. Moller, T. Gudnason, K. G. Kristinsson, U. Thorsteinsdottir and K. Stefansson (2020). "Spread of SARS-CoV-2 in the Icelandic Population." N Engl J Med **382**(24): 2302-2315.

Hall, R. N., A. Jones, E. Crean, V. Marriott, N. Pingault, A. Marmor, T. Sloan-Gardner, K. Kennedy, K. Coleman, V. Johnston and B. Schwessinger (2023). "Public health interventions successfully mitigated multiple incursions of SARS-CoV-2 Delta variant in the Australian Capital Territory." Epidemiol Infect **151**: e30.

Harris, S. R., E. J. Cartwright, M. E. Torok, M. T. Holden, N. M. Brown, A. L. Ogilvy-Stuart, M. J. Ellington, M. A. Quail, S. D. Bentley, J. Parkhill and S. J. Peacock (2013). "Whole-genome sequencing

for analysis of an outbreak of meticillin-resistant Staphylococcus aureus: a descriptive study." Lancet Infect Dis **13**(2): 130-136.
Hjorleifsson, K. E., S. Rognvaldsson, H. Jonsson, A. B. Agustsdottir, M. Andresdottir, K. Birgisdottir, O. Eiriksson, E. S. Eythorsson, R. Fridriksdottir, G. Georgsson, K. R. Gudmundsson, A. Gylfason, G. Haraldsdottir, B. O. Jensson, A. Jonasdotti, A. Jonasdottir, K. S. Josefsdottir, N. Kristinsdottir, B. Kristjansdottir, T. Kristjansson, D. N. Magnusdottir, R. Palsson, L. le Roux, G. M. Sigurbergsdottir, A. Sigurdsson, M. I. Sigurdsson, G. Sveinbjornsson, E. A. Thorarensen, B. Thorbjornsson, M. Thordardottir, A. Helgason, H. Holm, I. Jonsdottir, F. Jonsson, O. T. Magnusson, G. Masson, G. L. Norddahl, J. Saemundsdottir, P. Sulem, U. Thorsteinsdottir, D. F. Gudbjartsson, P. Melsted and K. Stefansson (2022). "Reconstruction of a large-scale outbreak of SARS-CoV-2 infection in Iceland informs vaccination strategies." Clin Microbiol Infect **28**(6): 852-858.
Houwaart, T., S. Belhaj, E. Tawalbeh, D. Nagels, Y. Frohlich, P. Finzer, P. Ciruela, A. Sabria, M. Herrero, C. Andres, A. Anton, A. Benmoumene, D. Asskali, H. Haidar, J. von Dahlen, J. Nicolai, M. Stiller, J. Blum, C. Lange, C. Adelmann, B. Schroer, U. Osmers, C. Grice, P. P. Kirfel, H. Jomaa, D. Strelow, L. Hulse, M. Pigulla, P. Kreuzer, A. Tyshaieva, J. Weber, T. Wienemann, M. Kohns Vasconcelos, K. Hoffmann, N. Lubke, S. Hauka, M. Andree, C. J. Scholz, N. Jazmati, K. Gobels, R. Zotz, K. Pfeffer, J. Timm, L. Ehlkes, A. Walker, A. T. Dilthey, C.-O. I. German and C.-O. I. German (2022). "Integrated genomic surveillance enables tracing of person-to-person SARS-CoV-2 transmission chains during community transmission and reveals extensive onward transmission of travel-imported infections, Germany, June to July 2021." Euro Surveill **27**(43).
Katoh, K. and D. M. Standley (2013). "MAFFT multiple sequence alignment software version 7: improvements in performance and usability." Mol Biol Evol **30**(4): 772-780.
Krause, G., D. Altmann, D. Faensen, K. Porten, J. Benzler, T. Pfoch, A. Ammon, M. H. Kramer and H. Claus (2007). "SurvNet electronic surveillance system for infectious disease outbreaks, Germany." Emerg Infect Dis **13**(10): 1548-1555.
Lane, C. R., N. L. Sherry, A. F. Porter, S. Duchene, K. Horan, P. Andersson, M. Wilmot, A. Turner, S. Dougall, S. A. Johnson, M. Sait, A. Goncalves da Silva, S. A. Ballard, T. Hoang, T. P. Stinear, L. Caly, V. Sintchenko, R. Graham, J. McMahon, D. Smith, L. E. Leong, E. M. Meumann, L. Cooley, B. Schwessinger, W. Rawlinson, S. J. van Hal, N. Stephens, M. Catton, C. Looker, S. Crouch, B. Sutton, C. Alpren, D. A. Williamson, T. Seemann and B. P. Howden (2021). "Genomics-informed responses in the elimination of COVID-19 in Victoria, Australia: an observational, genomic epidemiological study." Lancet Public Health **6**(8): e547-e556.
Leclerc, Q. J., N. M. Fuller, L. E. Knight, C. C.-W. Group, S. Funk and G. M. Knight (2020). "What settings have been linked to SARS-CoV-2 transmission clusters?" Wellcome Open Res **5**: 83.
Manica, M., P. Poletti, S. Deandrea, G. Mosconi, C. Ancarani, S. Lodola, G. Guzzetta, V. d'Andrea, V. Marziano, A. Zardini, F. Trentini, A. Odone, M. Tirani, M. Ajelli and S. Merler (2023). "Estimating SARS-CoV-2 transmission in educational settings: A retrospective cohort study." Influenza Other Respir Viruses **17**(1): e13049.
Mate, S. E., J. R. Kugelman, T. G. Nyenswah, J. T. Ladner, M. R. Wiley, T. Cordier-Lassalle, A. Christie, G. P. Schroth, S. M. Gross, G. J. Davies-Wayne, S. A. Shinde, R. Murugan, S. B. Sieh, M. Badio, L. Fakoli, F. Taweh, E. de Wit, N. van Doremalen, V. J. Munster, J. Pettitt, K. Prieto, B. W. Humrighouse, U. Stroher, J. W. DiClaro, L. E. Hensley, R. J. Schoepp, D. Safronetz, J. Fair, J. H. Kuhn, D. J. Blackley, A. S. Laney, D. E. Williams, T. Lo, A. Gasasira, S. T. Nichol, P. Formenty, F. N. Kateh, K. M. De Cock, F. Bolay, M. Sanchez-Lockhart and G. Palacios (2015). "Molecular Evidence of Sexual Transmission of Ebola Virus." N Engl J Med **373**(25): 2448-2454.
McCrone, J. T., V. Hill, S. Bajaj, R. E. Pena, B. C. Lambert, R. Inward, S. Bhatt, E. Volz, C. Ruis, S. Dellicour, G. Baele, A. E. Zarebski, A. Sadilek, N. Wu, A. Schneider, X. Ji, J. Raghwani, B. Jackson, R. Colquhoun, A. O'Toole, T. P. Peacock, K. Twohig, S. Thelwall, G. Dabrera, R. Myers, C.-G. U. Consortium, N. R. Faria, C. Huber, Bogoch, II, K. Khan, L. du Plessis, J. C. Barrett, D. M. Aanensen, W. S. Barclay, M. Chand, T. Connor, N. J. Loman, M. A. Suchard, O. G. Pybus, A. Rambaut and M. U. G.

Kraemer (2022). "Context-specific emergence and growth of the SARS-CoV-2 Delta variant." Nature **610**(7930): 154-160.
Mellmann, A., S. Bletz, T. Boking, F. Kipp, K. Becker, A. Schultes, K. Prior and D. Harmsen (2016). "Real-Time Genome Sequencing of Resistant Bacteria Provides Precision Infection Control in an Institutional Setting." J Clin Microbiol **54**(12): 2874-2881.
Mossong, J., N. Hens, M. Jit, P. Beutels, K. Auranen, R. Mikolajczyk, M. Massari, S. Salmaso, G. S. Tomba, J. Wallinga, J. Heijne, M. Sadkowska-Todys, M. Rosinska and W. J. Edmunds (2008). "Social contacts and mixing patterns relevant to the spread of infectious diseases." PLoS Med **5**(3): e74.
Nicolai, J., A. J. Miller, N. Hahn, J. Fazaal, A. Bunte, J. Silvery, M. Rosenstengel, P. Hoffmann, K. U. Ludwig, C. Tiemann, L. E. Rose and A. T. Dilthey (2025). "Large-scale SARS-CoV-2 sequencing indicates prior community circulation of the viral strain associated with Germany's largest meat processing plant." Sci Rep **15**(1): 38466.
Phuong, H. T., A. Bartz, A. K. Jarynowski, B. Lange, C. I. Jarvis, N. Rubsamen, R. T. Mikolajczyk, S. Scholz, T. Berger, T. Heinsohn, V. Belik, A. Karch and V. K. Jaeger (2025). "Changes in social contact patterns in Germany during the SARS-CoV-2 pandemic - an analysis based on the COVIMOD study." BMC Infect Dis **25**(1): 588.
Pullano, G., E. Valdano, N. Scarpa, S. Rubrichi and V. Colizza (2020). "Evaluating the effect of demographic factors, socioeconomic factors, and risk aversion on mobility during the COVID-19 epidemic in France under lockdown: a population-based study." Lancet Digit Health **2**(12): e638-e649.
Rambaut, A., E. C. Holmes, A. O'Toole, V. Hill, J. T. McCrone, C. Ruis, L. du Plessis and O. G. Pybus (2020). "A dynamic nomenclature proposal for SARS-CoV-2 lineages to assist genomic epidemiology." Nat Microbiol **5**(11): 1403-1407.
Rodiah, I., P. Vanella, A. Kuhlmann, V. K. Jaeger, M. Harries, G. Krause, A. Karch, W. Bock and B. Lange (2023). "Age-specific contribution of contacts to transmission of SARS-CoV-2 in Germany." Eur J Epidemiol **38**(1): 39-58.
Ryu, S., D. Kim, J. S. Lim, S. T. Ali and B. J. Cowling (2022). "Serial Interval and Transmission Dynamics during SARS-CoV-2 Delta Variant Predominance, South Korea." Emerg Infect Dis **28**(2): 407-410.
Seemann, T., C. R. Lane, N. L. Sherry, S. Duchene, A. Goncalves da Silva, L. Caly, M. Sait, S. A. Ballard, K. Horan, M. B. Schultz, T. Hoang, M. Easton, S. Dougall, T. P. Stinear, J. Druce, M. Catton, B. Sutton, A. van Diemen, C. Alpren, D. A. Williamson and B. P. Howden (2020). "Tracking the COVID-19 pandemic in Australia using genomics." Nat Commun **11**(1): 4376.
Shu, Y. and J. McCauley (2017). "GISAID: Global initiative on sharing all influenza data - from vision to reality." Euro Surveill **22**(13).
Sivertsen, A., N. Mortensen, U. Solem, E. Valen, M. F. Bullita, K. A. Wensaas, S. Litleskare, G. Rortveit, H. M. S. Grewal and E. Ulvestad (2024). "Comprehensive contact tracing during an outbreak of alpha-variant SARS-CoV-2 in a rural community reveals less viral genomic diversity and higher household secondary attack rates than expected." mSphere **9**(8): e0011424.
Walker, A., T. Houwaart, P. Finzer, L. Ehlkes, A. Tyshaieva, M. Damagnez, D. Strelow, A. Duplessis, J. Nicolai, T. Wienemann, T. Tamayo, M. Kohns Vasconcelos, L. Hulse, K. Hoffmann, N. Lubke, S. Hauka, M. Andree, M. P. Daumer, A. Thielen, S. Kolbe-Busch, K. Gobels, R. Zotz, K. Pfeffer, J. Timm, A. T. Dilthey and C.-O. I. German (2022). "Characterization of Severe Acute Respiratory Syndrome Coronavirus 2 (SARS-CoV-2) Infection Clusters Based on Integrated Genomic Surveillance, Outbreak Analysis and Contact Tracing in an Urban Setting." Clin Infect Dis **74**(6): 1039-1046.
Wong, N. S., S. S. Lee, T. H. Kwan and E. K. Yeoh (2020). "Settings of virus exposure and their implications in the propagation of transmission networks in a COVID-19 outbreak." Lancet Reg Health West Pac **4**: 100052.